



UNIVERSITY OF LEEDS

This is a repository copy of *The Ability of Quercetin and Ferulic Acid to Lower Stored Fat is Dependent on the Metabolic Background of Human Adipocytes*.

White Rose Research Online URL for this paper:

<https://eprints.whiterose.ac.uk/214733/>

Version: Accepted Version

Article:

Little, R., Houghton, M.J., Carr, I.M. orcid.org/0000-0001-9544-1068 et al. (3 more authors) (2020) The Ability of Quercetin and Ferulic Acid to Lower Stored Fat is Dependent on the Metabolic Background of Human Adipocytes. *Molecular Nutrition & Food Research*, 64 (12). 2000034. ISSN 1613-4125

<https://doi.org/10.1002/mnfr.202000034>

Reuse

Items deposited in White Rose Research Online are protected by copyright, with all rights reserved unless indicated otherwise. They may be downloaded and/or printed for private study, or other acts as permitted by national copyright laws. The publisher or other rights holders may allow further reproduction and re-use of the full text version. This is indicated by the licence information on the White Rose Research Online record for the item.

Takedown

If you consider content in White Rose Research Online to be in breach of UK law, please notify us by emailing eprints@whiterose.ac.uk including the URL of the record and the reason for the withdrawal request.



eprints@whiterose.ac.uk
<https://eprints.whiterose.ac.uk/>

MNFR

The ability of quercetin and ferulic acid to lower stored fat is dependent on the metabolic background of human adipocytes

Robert Little¹, Michael J. Houghton^{1,2}, Ian Carr³, Martin Wabitsch⁴, Asimina Kerimi^{1,2}, Gary Williamson^{1,2*}

¹School of Food Science and Nutrition, University of Leeds, Woodhouse Lane, Leeds, LS2 9JT, UK

²Department of Nutrition, Dietetics and Food, School of Clinical Sciences at Monash Health, Faculty of Medicine, Nursing and Health Sciences, Monash University, BASE Facility, 264 Ferntree Gully Road, Notting Hill, VIC 3168, Australia

³Saint James' University Hospital, Granville Road, Leeds, LS9 7TF, UK

⁴Department of Paediatrics and Adolescent Medicine, University Medical Centre, University of Ulm, 89075 Ulm, Germany

*Corresponding author. Phone: +61 3 99056649. Email: gary.williamson1@monash.edu

Running Title: Polyphenols reduce adipocyte lipid storage

Keywords: SGBS, gene expression, lipogenesis, LXR/RXR, nuclear receptors

ABBREVIATIONS

ACAT2	Acetyl-CoA acetyltransferase 2
ADH4	Alcohol dehydrogenase 4
ATP1A2	ATPase Na ⁺ /K ⁺ transporting subunit alpha 2
CD36	Cluster of differentiation 36, fatty acid translocase
CE	Cholesteryl esters
CYP4B1	Cytochrome P450 B1
DAG	Diacylglycerols/diglycerides
DCER	Dihydroceramides
FASN	Fatty acid synthase
(F)FA	(Free) fatty acids
FKBP5	FK506 (tacrolimus) binding protein 5
Fr A	Ferulic acid
HCER	Hexosylceramides
HMGCR	3-hydroxy-3-methyl-glutaryl-CoA reductase
HSD17B6	Hydroxysteroid 17-beta dehydrogenase 6
IPA	Ingenuity pathway analysis
LPC	Lysophosphatidylcholines
LPL	Lipoprotein lipase
LXR	Liver X receptor
MAG	Monoacylglycerols/monoglycerides
MAP2K6	Mitogen-activated protein kinase kinase 6
MVD	Mevalonate diphosphate decarboxylase
NFATC2	Nuclear factor of activated T cells 2
ORO	Oil Red O
PC	Phosphatidylcholines
PE	Phosphatidylehanolamine
PPAR	Peroxisome proliferator-activated receptor
PRKAR2B	Protein kinase cAMP-dependent type II regulatory protein beta subunit
PTGER3	Prostaglandin E receptor 3
Q	Quercetin
RNA-seq	RNA sequencing
RXR	Retinoid X receptor

SEM	Standard error of the mean
SGBS	Simpson-Golabi-Behmel syndrome
T3	Triiodothyronine
TAG	Triacylglycerols/triglycerides

“Ongoing lipogenic state”: differentiated human SGBS adipocytes containing stored lipids under conditions where they are actively making and accumulating additional lipids

“Lipid storage state”: differentiated human SGBS adipocytes containing stored lipids under conditions where, in the absence of external modulators, they are maintaining but not increasing stored lipids

1 **ABSTRACT**

2 **Scope:** Dietary flavonoids and phenolic acids can modulate biomarkers of lipid metabolism.

3 **Materials and methods:** Differentiated human SGBS adipocytes containing stored lipids,
4 mimicking white adipose tissue, were cultured either under conditions where they are
5 actively making and accumulating additional lipids through lipogenesis (“ongoing lipogenic
6 state”) or under conditions of maintaining but not increasing stored lipids (“lipid storage
7 state”). The cells were assessed for total lipids, by lipidomic analysis, and by transcriptomics.
8 In the “lipid storage state”, longer-term treatment with multiple low doses of quercetin,
9 ferulic acid or both together significantly reduced stored lipid content, modified genes
10 relating to lipid metabolism, with a strong implication of PPAR α /RXR α , and altered lipid
11 composition. In the “ongoing lipogenic state”, a higher concentration of quercetin was
12 required to attenuate stored lipid content, with no effect of ferulic acid, and there were fewer
13 changes in gene expression, no detectable involvement of PPAR α /RXR α , and fewer changes
14 in lipid composition.

15 **Conclusions:** Chronic low-dose treatment of quercetin and ferulic acid modulates lipid
16 metabolism in adipocytes, but the effect is dramatically dependent on the metabolic state of
17 the cell.

18 INTRODUCTION

19 The utilisation of stored lipids from white adipose tissue is a vital part of deriving energy for
20 human activity (1), but excessive storage of triglycerides is related to increased risk of
21 adverse cardiovascular events and developing type 2 diabetes (2). Flavonoids such as
22 quercetin protect against metabolic dysfunction in rodent high-fat diet models (3-5), and
23 against diabetic symptoms in streptozotocin-treated rats (6). The phenolic acid, ferulic acid,
24 can reduce the body weight of high fat diet-fed mice (7, 8). The effects of quercetin and
25 ferulic acid on adipocytes may be partially mediated via the gut microbiota (4) and via
26 hormonal and inflammatory processes (7), although key signalling pathways within
27 adipocytes remain to be elucidated.

28

29 *In vitro* cellular studies using murine-derived cell lines have shown that incubation with high
30 concentrations of (poly)phenols (which include flavonoids and phenolic acids, for
31 nomenclature see Frank et al 2019 (9)) can slow, or even prevent, the differentiation of pre-
32 adipocytes towards functionally mature lipid-storing cells (10-13). Triacylglycerol (TAG)
33 content was lower in murine 3T3-L1 adipocytes after several doses of quercetin during
34 differentiation, but no further mechanistic experiments were performed (13). Quercetin has
35 been proposed to directly affect mitochondrial processes, after significantly changing the
36 expression of adipokine- and glycolysis-related genes in human Simpson-Golabi-Behmel
37 syndrome (SGBS) adipocytes (14), and was shown to dose-dependently attenuate tumor
38 necrosis factor α (TNF α)-mediated inflammation in 3T3-L1 adipocytes (15). Oral
39 administration of ferulic acid to rodents on a high-fat diet significantly reduced expression of
40 fetuin-A, involved in lipid-induced adipocyte inflammation, and pro-inflammatory cytokines
41 in adipose and circulation (7, 15). Ferulic acid at high concentration also attenuated 3T3-L1

42 adipogenesis via heme oxygenase-1 regulation (16). Crucially, the chronic effect and
43 mechanism of action on differentiated adipocytes remains unknown.

44

45 We report here the effects of repeated treatments over 3 d of low concentrations of quercetin
46 and/or ferulic acid on matured human SGBS adipocytes under conditions where they are
47 synthesising lipid, as a model for the effect on lipogenesis, or storing lipid, where the process
48 of fat utilisation, predominantly through fatty acid β -oxidation, becomes predominant.

49 **MATERIALS AND METHODS**

50 **Materials**

51 Preadipocyte cells of the Simpson-Golabi-Behmel syndrome (SGBS) strain originate from
52 adipose tissue of a young patient with SGBS. These cells have been previously characterised
53 (17-19). All reagents were purchased from Sigma-Aldrich, UK, unless otherwise stated, and
54 were of the highest analytical grade available. A solution of 3.3 mM pantothenate with 1.7
55 mM biotin (termed pan-bio) was prepared in DMEM/F-12 medium (25 mM glucose) (Gibco,
56 UK). Quercetin (Extrasynthese, France) and ferulic acid (Sigma-Aldrich) were prepared as
57 master stock solutions of 50 mM in DMSO and stored in small aliquots at -20°C until
58 required. A solution of 3% (w/v) Oil Red O was prepared using PBS and was stored at 4°C
59 for up to 12 months.

60

61 **Culture of SGBS cells**

62 SGBS cells of passages 31-41 were used in this study and were routinely cultured in T175
63 tissue culture vessels (Corning, UK). Cell proliferation was promoted by culturing under
64 DMEM/F-12 medium (25 mM glucose) supplemented with 1% (v/v) penicillin-streptomycin
65 solution, 1% (v/v) pan-bio solution (to comprise basal medium) and 10% (v/v) fetal bovine
66 serum (source: South America, Gibco, UK) (to comprise growth medium). Cells were
67 incubated in a humidified atmosphere of 37°C and 5% CO₂, were routinely cultured every 3-4
68 d and passaged with trypsin. Pre-adipocyte SGBS cells were promoted to differentiate as
69 previously described (18). In summary, SGBS cells were plated at a density of 3×10^3 cells
70 cm⁻² and incubated in growth medium for 4 d. Differentiation was initiated by incubation in
71 basal medium supplemented with 125 nM transferrin, 20 nM human insulin, 100 nM cortisol,
72 0.2 nM triiodothyronine (T3), 25 nM dexamethasone, 250 μM 3-isobutyl-1-methylxanthin
73 (IBMX) and 2 μM rosiglitazone (Cayman Chemicals, Cambridge Bioscience, UK)

74 (adipogenic medium) for 4 d. Subsequent lipogenesis was promoted by incubation in basal
75 medium supplemented with only transferrin, insulin, cortisol and T3 for 10 d, with the
76 medium being newly refreshed twice (**Fig. 1**). Cultured cells were visualised using a Leica
77 MD IL LED inverted brightfield microscope (Leica Microsystems, Germany) and imaged
78 with LAS X software (Leica Microsystems).

79

80 **Cellular uptake of radiolabelled 2-deoxy-D-glucose**

81 SGBS cells were cultured on 12-well tissue culture plates (Corning) and promoted to
82 differentiate for a total of 14 d as described above. Cells were incubated in DMEM/F-12 for 4
83 h without insulin before incubation with 0.55 mM deoxy-D-glucose (0.27 mCi/ml 2-[1-
84 ¹⁴C(U)]-deoxy-D-glucose (PerkinElmer, UK)) in DMEM/F-12 (with no glucose) with vehicle
85 (DMSO) or 20 nM insulin for 30 min. Cells were then washed twice in DMEM/F-12 (with no
86 glucose), lysed in 1M NaOH and then neutralised with 1M HCl. Treatments were performed
87 in duplicate wells and pooled. Isotope activity was determined by liquid scintillation counting
88 (Tri-Carb 1900 TR Liquid Scintillation Analyzer, Canberra Packard, UK). Obtained counts
89 per min were corrected for total protein, measured in aliquots of the lysates using the
90 Bradford assay (Pierce Bradford Protein Assay Kit, Thermo Fisher Scientific, UK).

91

92 **Treatment of SGBS cells with (poly)phenols**

93 Maturing SGBS cells (14 d culture) were treated with vehicle (DMSO), quercetin or ferulic
94 acid or a combined quercetin and ferulic acid treatment at time zero and every 24 h for up to
95 48 h (Time = 0, 24 and 48 h) as shown in **Fig. 1**. Treatments were applied as additions to
96 basal media (cells in “lipid storage state”) or to lipogenic media (ongoing lipogenesis).

97

98 **Detection of lipid accumulation by Oil Red O staining**

99 SGBS cells were cultured on 12-well plates, and following treatment, the medium was
100 removed and cells washed with warmed PBS before being incubated at room temperature in
101 4% paraformaldehyde for 30 min. Subsequently the fixative solution was removed and the
102 cells washed twice in PBS before being stored under PBS at 4°C until required. PBS was
103 removed and fixed cells were immersed for 30 min in an Oil Red O (ORO) staining solution,
104 prepared by diluting 3:2 stock solution to milliQ water (Merck-Millipore, UK). The cells
105 were subsequently washed twice in water and once in PBS, then air-dried at room
106 temperature. The stain was solubilised by covering the monolayer in isopropanol for 5 min.
107 Samples from each well were collected and diluted 4-fold in isopropanol with a 100 µL
108 aliquot transferred to a clear bottomed 96-well plate (Corning). The absorbance of each
109 sample between 440 and 600 nm was measured using a PHERAStar FS plate reader (BMG
110 LabTech, Germany) with maximal absorbance at 514 nm used for analysis.

111

112 **Detection of free glycerol**

113 SGBS were plated, differentiated and treated as described above. On the third treatment day
114 at T = 72 h, 24 h after the final treatment, conditioned media was collected. The amount of
115 free glycerol was determined using a cell-based assay kit (Cayman Chemicals) according to
116 the manufacturer's protocol. Samples and standards were assayed using technical duplicates
117 in a 96-well plate (Nunc, Thermo Fisher Scientific) and absorbance at 540 nm was
118 determined by PHERAStar FS plate reader. The amount of free glycerol in treated samples
119 was calculated by subtracting mean A_{540} values of control with no glycerol with glycerol
120 reagent free controls (media only) from the mean value of the treatment, relative to a standard
121 curve.

122

123 **Determination of lipid species by mass spectrometry**

124 Cells were propagated in T75 tissue culture flasks and treated as shown in **Figure 1**. Four
125 flasks received each treatment and were subsequently pooled as a single sample. All samples
126 were collected at 72 h, 24 h after the final treatment. Cells in each flask were washed with
127 warmed PBS and were liberated by trypsin (5 min, 37°C, 5% CO₂). An aliquot (10 µL) was
128 collected and live cell number determined by automatic cell count (TC20, Bio-Rad, UK)
129 using trypan blue. Cells were pelleted from suspension by centrifugation at 200 × g for 5 min,
130 and were promptly snap frozen in liquid nitrogen before being stored at -80°C. Cell pellets
131 were resuspended in deionised water and homogenised by ultrasonication. A small aliquot of
132 homogenate was removed and used to determine total protein amount by Bradford assay for
133 subsequent normalisation of lipid species. The remainder of each homogenate was subjected
134 to a modified Bligh-Dyer extraction with extracts being dried under nitrogen and
135 reconstituted in ammonium acetate dichloromethane:methanol. The extracts were transferred
136 to vials for infusion LC-MS/MS (liquid chromatography/mass spectrometry), performed on a
137 Shimadzu LC with nanopolyetheretherketone tubing and the SCIEX SelexIon-5500 triple
138 quadrupole linear ion trap (QTRAP). The samples were analysed via both positive and
139 negative mode electrospray. The 5500 QTRAP was operated in multiple reaction monitoring
140 (MRM) mode with a total of more than 1,100 MRMs (Metabolon, Potsdam,
141 Germany). Individual lipid species were quantified by taking the ratio of the signal intensity
142 of each target compound to that of its assigned internal standard, then multiplying by the
143 concentration of internal standard added to the sample. Lipid class concentrations
144 were calculated from the sum of all molecular species within a class, and fatty acid
145 compositions were determined by calculating the proportion of each class comprised by
146 individual fatty acids. Concentrations are expressed as nmol of lipid per mg protein in the
147 sample.

148

149 **Transcriptomics analysis**

150 Cells were treated as described above and detailed in **Figure 1**, but all samples were collected
151 at T = 54 h. The wells were washed with PBS and lysed with Lysis/Binding Solution
152 (Invitrogen, Thermo Fisher Scientific). Three wells per treatment were combined for each
153 sample and samples were stored at -80°C until required. A volume of 100% ethanol equal to
154 the collected volume was added to each sample and total RNA was extracted using an Aurum
155 Total RNA mini kit (Bio-Rad) as per the manufacturer's instructions. Isolated nucleic acids
156 were quantified by Nanodrop (ND-1000, LabTech International, UK), with all analysed
157 samples exhibiting a A_{260}/A_{280} ratio exceeding 1.9, and stored at -80°C. Total RNA (100 ng)
158 was used to generate Illumina-compatible stranded, polyA selected, RNA-seq (RNA-
159 sequencing) libraries using the TruSeq Stranded Total RNA Library Kit (Illumina, USA). The
160 resultant libraries were quantified on the TapeStation automated electrophoresis tool (Agilent
161 Technologies, USA) and Qubit fluorometer (Thermo Fisher Scientific) before pooling to
162 create an equimolar pool that was sequenced on an Illumina NextSeq 75 bp single end read
163 lane. Adaptor sequences and low-quality base calls were removed using Cutadapt software
164 (20) and the quality of the data determined using FastQC tool (Babraham Bioinformatics,
165 Babraham Institute, UK). The data was aligned to the human genome (hg38) using STAR,
166 the ultra-fast universal RNA-seq aligner (21), with reference to the RefSeq gene annotation
167 database (22), which was obtained from the University of California, Santa Cruz, Genome
168 Browser website (23). Binary alignment map (BAM) files containing the aligned data ordered
169 by genomic position where indexed using the SAMtools sequence alignment/map tool
170 program suite (24) and PCR duplicates were marked using the Picard genome analysis toolkit
171 (25). The aligned data quality was then determined using the Qualimap software (26). As
172 there were no issues with DNA contamination or PCR duplicates, the Rsubread software
173 package (27) was used to count reads mapping to each RefSeq transcript. Differentially

174 expressed transcripts were identified using the R package DeSeq2 (28). Transcripts with a p
175 value, adjusted for multiple testing, of less than 0.05 were identified as differentially
176 expressed.

177

178 **Analyses and statistical approaches**

179 Quantification of lipid deposition was carried out on 96-well plates, run in triplicate at 514
180 nm using isopropanol as a dilution control. The effect of (poly)phenol treatments was
181 assessed by the students' t -test for each treatment against vehicle treatment with level of
182 significance set at $p < 0.05$. Analysis and presentation of MS data was performed using the
183 Metabolon SurveyorTM online tool. Pathway and gene analysis from the transcriptomics data
184 was performed using the Qiagen Ingenuity Pathway Analysis (IPA) tool (QIAGEN Inc.,
185 Netherlands (29)). The algorithms developed for IPA are detailed by Krämer and colleagues
186 (30). The relevance of gene expression to a pathway or disease was scored by Fishers Exact
187 Test p -value. A level of significance of $p < 0.001$ was set for the relationship of pathways to
188 diseases and metabolic functions. Data are presented as mean values \pm the standard error of
189 the mean (SEM).

190 RESULTS

191 Establishing conditions of lipid storage and ongoing lipogenesis

192 Promoting differentiation of SGBS cells induced a change in morphology from day 4 with
193 some intracellular lipid deposits visible by microscopy from day 8 (**Fig. 2A**), clearly evident
194 after 14 d, and further increasing to day 17 (**Fig. 2B**). The storage of neutral intracellular lipid
195 was confirmed by Oil Red O staining (**Fig. 2B**). SGBS cells displayed a significant insulin-
196 sensitive component of 2-[1-¹⁴C(U)]-deoxy-D-glucose uptake (**Fig. 2C**). From day 14 to 17,
197 there was a significant increase in the amount of lipid present in the cells under continued
198 presence of the differentiation medium (“ongoing lipogenic state”), but not if the cells were
199 cultured in basal media between days 14 and 17, when the intracellular stored lipid remained
200 constant (“lipid storage state”) (**Fig. 2D**).

201

202 Cells at days 14-17 were used for experiments, in either the “ongoing lipogenic state” or
203 “lipid storage state”, during which they were treated with one or more doses of quercetin,
204 ferulic acid or both, and compared to vehicle control. Cell number (**Fig. 3A**) and viability
205 (**Fig. 3B**) were not affected over this time by 3 repeated 24 h treatments of 1 μ M quercetin, 1
206 μ M ferulic acid or both compounds combined. For lipidomic analysis, 5 biological replicates,
207 with each derived from 4 pooled T75 flasks, were analysed. The time-point analysed was 72
208 h, i.e. 24 h after the final treatment (**Fig. 1**). For transcriptome analysis, 4 replicates were
209 initially performed but only 3 met the quality criteria; these 3 samples were subsequently
210 analysed and showed limited batch variation (**Fig. 4A**). The time-point analysed was 54 h, i.e.
211 6 h after the final treatment (**Fig. 1**). Whether a transcript was significantly altered by
212 treatment was independent of the level of expression of that transcript (**Fig. 4B**). Principal
213 component (PC) analysis (PCA) showed that 2 factors could clearly separate the dataset for
214 each treatment and account for $\geq 95\%$ of the full variation. Principal component 1 contributed

215 very strongly to the separation (**Fig. 4C**) and all treatments represented a minimum of 85% of
216 variance.

217

218 **Comparison of untreated SGBS cells in the “lipid storage state” to “ongoing lipogenic** 219 **state”**

220 When cells in the “ongoing lipogenic state” were compared to those in the “lipid storage
221 state” at 54 h, 422 transcripts were significantly upregulated and 388 were downregulated.

222 The most highly upregulated transcripts included CYP4B1 (cytochrome P450 B1) (\log_{10} ratio
223 = 4.51), ATP1A2 (ATPase Na⁺/K⁺ transporting subunit alpha 2) (4.25), FKBP5 (FK506

224 binding protein 5) (3.21), MAP2K6 (mitogen-activated protein kinase kinase 6) (2.92) and

225 MVD (mevalonate diphosphate decarboxylase) (2.34), and the most highly downregulated

226 transcripts included HSD17B6 (hydroxysteroid 17- β dehydrogenase 6) (-2.52), SLC7A14

227 (solute carrier family 7, member 14) (-2.31) and transcription factor POU2F2 (POU (Pit-Oct-

228 Unc) class 2 homeobox 2) (-2.26). Lipidomic analysis revealed a total of 1047 intracellular

229 lipid species, and showed that cells in an “ongoing lipogenic state” exhibited some

230 differences in lipid profile after 72 h compared to cells in the “lipid storage state”. The former

231 showed an almost 6-fold decrease in the proportion of monoacylglycerol MAG (22:0),

232 together with some increases in the proportions of various di- and triacylglycerol species

233 (**Fig. 5**). For total lipid classes, only the hexosylceramides (HCER) were significantly

234 different (31.4%; $p = 0.0369$).

235

236 **Effects of treatment of SGBS adipocytes in a “lipid storage state”**

237 The treatment of 3 \times 24 h repeated doses of 1 μ M quercetin, 1 μ M ferulic acid or both

238 together over 3 d attenuated ORO-stained intracellular lipid content. The combination was

239 stronger than quercetin treatment alone ($p < 0.05$) or ferulic acid alone (trend, $p = 0.075$)

240 (Fig. 6A). Treatment with the same concentration for 2 × 24 h doses (Fig. 6B) or with a
241 single dose over 72 h (Fig. 6C) showed no significant effect on ORO-stained lipid content.
242 Media collected from 3 × 24 h treatments of 1 μM quercetin at the end of the 72-h incubation
243 period contained a significantly higher level of free glycerol compared to vehicle-treated
244 control cells (Fig. 6D).

245

246 The changes were examined further by mass spectrometry to quantify individual lipid
247 species. Treatment for 3 × 24 h doses of 1 μM quercetin, 1 μM ferulic acid, or both
248 combined, did not significantly affect the absolute concentration of any total lipid class, but
249 changed the lipid composition as indicated by the mole fraction of each class (Table 1). The
250 combined treatment produced more changes overall than the compounds individually. The
251 most notable effect seen by quercetin alone was a 75% reduction in the MAG (22:0) fraction
252 ($p < 0.01$), and with ferulic acid alone there was a 64% increase in the free fatty acids fraction
253 ($p < 0.05$). When combined, ferulic acid only mildly alleviated the effect of quercetin on
254 MAG (22:0) while quercetin completely annulled the ferulic acid-induced increase in the
255 proportion of free fatty acids (Table 1).

256

257 The effect of 3 × 24 h treatments on cells under “lipid storage conditions” on the number of
258 gene expression changes is summarised in Table 2. 71.3% of genes altered by quercetin
259 treatment were also affected by ferulic acid, and 92.8% of genes altered by ferulic acid were
260 also changed by the quercetin treatment. For the combined quercetin and ferulic acid
261 treatment, a proportion (41.3%) of genes were solely altered compared to the individual
262 treatments (Fig. 7A). When gene expression changes were analysed by ingenuity pathway
263 analysis (IPA), the general category of lipid metabolism exhibited the strongest association
264 for quercetin ($p = 8.74 \times 10^{-18}$) and for ferulic acid ($p = 1.98 \times 10^{-14}$). Combined treatment in

265 lipid storage conditions was also highly significantly associated with fatty acid metabolism (p
266 = 3.20×10^{-14}), and all treatments were strongly significantly related to multiple key
267 pathways and systems associated with lipid handling and development of obesity (**Fig. 7B**).
268 The effects of gene changes associated with quercetin treatment in lipid storage conditions
269 are predicted to significantly decrease the synthesis, accumulation and concentration of lipid
270 (**Fig. 7C**) (activation z-scores of -0.629, -0.889 and -2.370 respectively). The transcription
271 factor NFATC2 (nuclear factor of activated T cells 2) was also strongly significantly
272 increased by quercetin treatment. Expression changes due to ferulic acid treatment are
273 predicted to weakly increase synthesis of lipid (z-score 0.310) but to significantly reduce
274 concentration and accumulation of lipid (-1.468 and -0.635 respectively). Genes contributing
275 to these effects are displayed in **Fig. 7D**. Expression changes due to combined quercetin and
276 ferulic acid treatment are predicted to weakly increase synthesis of lipid (z-score 0.239) but
277 to significantly reduce concentration and accumulation of lipid (-1.406 and -0.941
278 respectively) (**Fig. 7E**). Notable gene changes, which are significantly associated with altered
279 lipid synthesis and/or storage with all treatments, are summarised in **Table 3**. Pathway
280 analysis of gene expression changes showed that the effects on lipid metabolism could be
281 linked to PPAR α /RXR α (peroxisome proliferator-activated receptor- α /retinoid receptor X- α)
282 signalling, inducing a predicted downregulation of lipid metabolism when treated with 1 μ M
283 quercetin (z-score = -2.111; $p = 4.8 \times 10^{-5}$) (**Fig. 7F**), 1 μ M ferulic acid (z-score = -1.00; $p =$
284 1.14×10^{-3}) (**Fig. 7G**) or both (z-score = -1.155; $p = 4.06 \times 10^{-4}$) (**Fig. 7H**).

285

286 **Effects of treatment of SGBS adipocytes during ongoing lipogenesis**

287 Treatment of SGBS with 3 \times 24 h repeated doses of 1 μ M quercetin, 1 μ M ferulic acid or
288 both showed no significant effect on ORO-stained neutral lipid accumulation under “ongoing
289 lipogenic conditions”, and only a 10-fold higher concentration of combined ferulic acid and

290 quercetin was effective (**Fig. 8A and B**). Lipids were analysed after 3 × 24 h repeated doses
291 of 1 μM quercetin, 1 μM ferulic acid or both, and in accord there was no significant effect on
292 the absolute concentration of any total lipid class (**Table 4**). However, all treatments
293 generally lowered the free fatty acid fractions, which was not observed in the “lipid storage
294 state”. Other notable changes in lipid composition include a shift to more unsaturated
295 triacylglycerol species, and an increase in ceramides, only with the individual quercetin and
296 ferulic acid treatments. Ferulic acid alone also induced a 5-fold increase in the PE (O-
297 16:0/18:2) fraction. The combined treatment lowered the relative saturated and mono-
298 unsaturated species, particularly the diacylglycerols, while there was a relatively large
299 reduction in the PC (18:0/14:1), seen only with the combination (**Table 4**).

300

301 For ferulic acid, 3 × 24 h repeated doses caused few changes in gene expression, but 3 × 24 h
302 repeated doses of 1 μM quercetin, and combined treatment, brought about more changes
303 (**Table 2**). 58.1% of genes altered by quercetin treatment were also altered in the combined
304 treatment (**Fig. 9A**). Lipid metabolism, small molecule biochemistry and metabolic disease
305 were notable modified functions, although the effect of ferulic acid treatment alone was small
306 (**Fig. 9B**). The effects of gene changes associated with quercetin treatment are predicted to
307 significantly decrease synthesis, conversion and accumulation of lipid (**Fig. 9C**) (activation z-
308 scores of -0.218, -0.453 and -0.264 respectively). Expression changes due to ferulic acid
309 treatment are predicted to significantly decrease conversion of lipid (-0.594), related to the
310 significantly reduced expression of ADH4 (alcohol dehydrogenase 4), HMGCR (3-hydroxy-
311 3-methyl-glutaryl-CoA reductase) and PTGER3 (prostaglandin E receptor 3). Other lipid
312 handling functions were not significantly affected by chronic 1 μM ferulic acid treatment.
313 Expression changes due to combined quercetin and ferulic acid treatment are predicted to
314 significantly decrease conversion of lipid (z-score -0.60), accumulation of lipid (z-score -

315 1.109) and concentration of lipid (z-score -1.328) (**Fig. 9D**). Notable gene changes in all
316 treatments that are significantly associated with altered lipid synthesis and/or storage are
317 summarised in **Table 5**.

318

319 Unlike in the “lipid storage state”, changes in gene expression in cells in an “ongoing
320 lipogenic state” did not significantly associate with the PPAR α /RXR α signalling canonical
321 pathway. Instead, the effects of quercetin and of combined quercetin and ferulic acid
322 treatments were most notably on the super-pathway of cholesterol biosynthesis (predicted
323 deactivation, z-score = -2.236, $P = 1.7 \times 10^{-7}$) and (-2.828, $P = 2.44 \times 10^{-10}$) respectively.
324 Reduced cholesterol biosynthesis activity was associated with significantly reduced
325 expression of ACAT2 (acetyl-CoA acetyltransferase 2, experimental log ratio = -0.797),
326 HMGCS1 (3-hydroxy-3-methyl-glutaryl-CoA synthase 1, -0.736) and HMGCR (-1.072) in
327 chronic quercetin-treated cells, and with ACAT2 (-0.716), HMGCR (-0.962), MSMO1
328 (methylsterol monooxygenase 1, -0.871) and NSDHL (NAD(P)-dependent steroid
329 dehydrogenase-like, -0.684) with combined treatment.

330 **DISCUSSION**

331 Differentiated SGBS cells behave as functional human adipocytes (17, 18) with a white
332 adipose tissue-like phenotype (19). By following a differentiation protocol in high glucose
333 (18), SGBS cells time-dependently synthesise and accumulate lipid. The cells were then
334 maintained under conditions where they continued to carry out lipogenesis and increased
335 their intracellular lipid, or under conditions where they maintained the stored lipid but did not
336 increase the content. In order for a treatment to lower the amount of stored lipid under “lipid
337 storage state” conditions, the process of fat utilisation, mostly through β -oxidation, would
338 need to be stimulated.

339

340 In the “ongoing lipogenic state”, compared to the “lipid storage state”, there was a substantial
341 decrease in the proportion of monoacylglycerol (22:0) species, with increases in various
342 DAG and TAG species, expected to be formed for adipocyte differentiation and fat storage
343 (31). An increase in the proportion of the hexosylceramide class is indicative of cell
344 membrane synthesis, while levels of hexosylceramides in adipose and liver are also linked to
345 metabolic syndrome, notably insulin resistance, oxidative stress and inflammation (32-34).
346 Upregulation of CYP4B1, ATP1A2, FKBP5, MAP2K6 and MVD transcripts are indicative
347 of the ongoing lipogenesis and relate to obesity development in vivo. CYP4B1 is a target of
348 PPAR activation (35) and is associated with increased lipid synthesis and adipose tissue
349 expansion, with substantial upregulation in obese pigs (36). Increased ATP1A2 indicates
350 plasma membrane increases and tissue expansion, and has been linked to hyperphagia in mice
351 (37). FKBP5 expression in human adipose is increased in T2D patients, relating to insulin
352 resistance and hyperglycaemia, and may be a key factor in glucocorticoid-induced insulin
353 resistance (38). MAP2K6 activates p38 MAP kinase in response to inflammatory cytokines
354 or stress, leading to stress-induced cell cycle arrest and apoptosis. Expression of this kinase is

355 elevated in the white adipose tissue of obese individuals, and its inhibition may promote
356 adipose tissue browning and increase organismal energy expenditure (39). MVD encodes
357 mevalonate diphosphate decarboxylase, which regulates an early step in cholesterol
358 biosynthesis. MVD was also found to be upregulated in mice treated with an anti-obesity
359 therapeutic (40) or a Utx (Ubiquitously transcribed tetratricopeptide repeat, X chromosome, a
360 regulator of lipid metabolism)-demethylase knockout (41), with reduced triacylglycerol
361 synthesis but increased cholesterol synthesis. Of the genes that were significantly
362 downregulated in the “ongoing lipogenic state”, notably the hepatic expression of HSD17B6
363 was also lowered in obese women (42).

364

365 In the “lipid storage state”, quercetin and ferulic acid, in addition to attenuating lipid content,
366 changed the lipid composition, with more changes occurring when quercetin and ferulic acid
367 were combined. From the transcriptomics data, functions related to lipid metabolism such as
368 lipid handling, lipid accumulation and obesity development, were consistently regulated, with
369 strong predicted negative activation z-scores. NFATC2, associated with lipid synthesis, was
370 upregulated by ferulic acid and by the combined treatment, while ABCA1, a regulator of
371 intracellular cholesterol and HCER (43), was downregulated. Together with the lipidomics
372 data, this may contribute to the lower lipid accumulation (44-46). Pathway analysis showed
373 that the regulated transcripts are predicted to be controlled by the PPARs, the master
374 regulators of adipogenesis (47, 48), specifically nuclear PPAR α and/or RXR α receptors, but
375 not PPAR γ . For all three (poly)phenol treatments, the PPAR α /RXR α -regulated genes
376 ABCA1, CD36 (cluster of differentiation 36/fatty acid translocase) and LPL (lipoprotein
377 lipase) genes were downregulated. The targeted deletion of ABCA1 in mouse adipocytes
378 decreased diet-induced obesity, lowering lipogenesis and triglyceride accumulation (44).
379 CD36 and LPL have roles in importing and promoting cellular uptake of free fatty acids (49)

380 and reduced expression of these three resultant proteins would be predicted to be associated
381 with reduced ability to accumulate and concentrate intracellular lipid. Overexpression of LPL
382 specifically in mouse skeletal muscle or liver has been shown to increase triacylglycerol
383 content in cells of these tissues (50), whilst CD36 has been proposed to have a regulatory
384 role in fat gustatory perception in humans (51). Quercetin also regulated FASN (fatty acid
385 synthase), and (poly)phenol supplementation has been shown to significantly reduce body
386 mass and fat pad mass of rats fed a high fat diet with an associated significantly reduced
387 expression of FASN mRNA (52). Ferulic acid regulated PRKAR2B (protein kinase cAMP-
388 dependent type II regulatory protein β -subunit), and genetic disruption of PRKAR2B in mice
389 has been shown to be linked with limited ability to gain weight on a high fat diet and
390 increased energy expenditure of the modified mammals (53).

391

392 Whilst we show that treatment of SGBS cells in the “lipid storage state” by three low doses
393 of quercetin, ferulic acid or both significantly reduced the amount of neutral lipids, much
394 higher concentrations were required to induce this effect in the “ongoing lipogenesis state”,
395 where lipogenesis is dominant. The PE (O-16:0/18:2) fraction was increased by ferulic acid,
396 and an increase in this species was similarly measured in the subcutaneous adipose tissue of
397 mice on a chow-fed diet versus those on a high-fat diet (54). Conversely, with quercetin and
398 ferulic acid, we also observed a shift in lipid composition towards more unsaturated TAGs
399 and non-storage lipids, seen in white adipose tissue of the mice following a high-fat diet (54),
400 and an increase in the ceramide fraction, which is commonly known to be associated with
401 metabolic syndrome risk (55). Nevertheless, our transcriptomics data suggest an overall
402 decrease in lipid synthesis, accumulation and conversion, gene expression changes consistent
403 with the super-pathway of cholesterol biosynthesis, rather than with PPAR α /RXR α signalling
404 as in the “lipid storage state”. Reduced cholesterol biosynthesis activity was associated with

405 quercetin, whether treated individually or combined, and AMP-activated protein kinase
406 (AMPK) signalling and reduced leptin expression was associated with ferulic acid. Overall,
407 these outcomes suggest a decrease in adipose expansion and lipid storage. Free fatty acid
408 fractions were decreased with all (poly)phenol treatments and this is associated with a lower
409 risk of insulin resistance, inflammation and metabolic syndrome (56).

410

411 In SGBS cells, a high concentration of quercetin (25 μ M) for 16 h induced strong
412 downregulation of mRNA for PFKFB, the gene for 6-phosphofructokinase isozyme 2, and the
413 PPAR-regulated ANGPTL4 gene product (angiopoietin-like 4) (14), a secreted protein
414 induced by glucocorticoids that inhibits LPL and stimulates intracellular adipocyte lipolysis
415 (57); taken together downregulation of these proteins may reduce the accumulation of free
416 fatty acids, and the associated lipotoxicity and inflammation, in insulin-resistant adipose
417 tissue. It has previously been reported that quercetin treatment during differentiation of pre-
418 adipocytes can reduce adipogenesis of murine 3T3-L1 murine cells (58). Relatively high *in*
419 *vivo* dosing regimens have been reported to promote anti-obesity effects in mice (3-5).

420 (Poly)phenols can also have other effects on adipose, where 3T3-L1 cells and rat adipose
421 tissue can be remodelled ('browned') to exhibit a more metabolically active brown-like
422 adipose cell phenotype (59, 60). Polyphenol treatment promoting adipocyte remodelling to a
423 brown cell-like phenotype has been shown to occur alongside changes in gene expression for
424 UCP1 (uncoupling protein 1), PPAR γ coactivator 1 α and FGF21 (fibroblast growth factor 21)
425 (59, 61). A consequence of browning may be increased triglyceride-derived fatty acid uptake
426 by white adipose (62).

427

428 In summary, (poly)phenols appear to more strongly enhance the burning of fat, but with
429 weaker effects on the synthesis of fat since in adipocytes that are actively making lipids, then

430 a much higher concentration is needed to lower the rate of synthesis. The effects on cells
431 storing lipid was through PPAR α /RXR α activation, but these transcription factors were not
432 involved in cells actively undergoing lipogenesis.

433 **Acknowledgments**

434 This research has received funding from the European Research Council Advanced grant
435 number 322467 (*'POLYTRUE?'*). The authors thank Metabolon (Potsdam, Germany) for
436 assessment of lipid species using mass spectrometry.

437

438 **Declarations of interest:** none.

439

440 **Author Contributions**

441 GW, AK and RL designed the study. RL performed experimental work, analysed data and
442 drafted the manuscript. MJH performed 2-deoxy-D-glucose uptake experiments, contributed
443 to experimental planning and interpretation of results, and helped draft the manuscript. IMC
444 performed transcriptome sequencing. MW provided essential tools (SGBS cells). AK
445 contributed to transcriptome analysis. GW and AK obtained funding. RL, MJH, AK and GW
446 edited the manuscript. All authors approve submission.

TABLES

Table 1: The effect of treatment on the mole fraction of lipid species in SGBS cells under “lipid storage state” conditions

Molecular Species	Quercetin	Ferulic Acid	Quercetin + ferulic acid	Affected by Differentiation
MAG (17:0)	N.S	N.S	90 *	no
MAG (22:0)	24.6 **	N.S	35.4 *	yes
TAG 48:0-FA 14:0	70.7 *	N.S	N.S	no
TAG 44:0-FA 16:0	N.S	77.9 *	N.S	yes
TAG 44:0-FA 12:0	N.S	75.0 *	75.0 *	yes
TAG 47:1-FA 17:0	N.S	78.6 *	N.S	no
FFA (14:1)	N.S	163.6 *	N.S	yes
PC (16:0/12:0)	N.S	N.S	65.0 *	no
PC (16:0/16:0)	N.S	N.S	123.6 *	yes
PC (16:0/18:0)	N.S	N.S	95.6 *	no
PC (16:0/18:3)	N.S	N.S	67.9 *	no
PC (17:0/18:2)	N.S	N.S	63.9 *	no
PC (18:1/20:5)	N.S	N.S	170.8 **	no
PC (18:2/18:3)	67.1 *	N.S	N.S	no
PC (18:2/22:6)	75.0 *	N.S	N.S	no
PE (O-16:0/20:4)	N.S	N.S	123.5 **	no
PE (P-16:0/20:4)	N.S	N.S	123.8 *	no
PE (16:0/22:6)	131.3 *	N.S	125.0 *	no
PE (18:0/20:1)	N.S	N.S	83.3 *	no
LPC (16:0)	N.S	85.8 *	N.S	no

The effect of treatment (all $3 \times 1 \mu\text{M}$ for 54 h) is expressed as a percentage of the vehicle control (100%). Mole fraction is the relative amount of a particular species as a percentage of all lipid species of that lipid class. All other detected metabolites (not listed) were not significantly affected by any treatment. n=5. N.S, not significant. * $p < 0.05$, ** $p < 0.01$, *** $p < 0.001$.

Table 2: Total number of transcripts regulated significantly

Treatment	Lipid storage state		Ongoing lipogenesis state	
	Expression	Expression	Expression	Expression
	increased	decreased	increased	decreased
1 μ M quercetin	216	84	140	87
1 μ M ferulic acid	211	96	33	12
1 μ M quercetin and ferulic acid	365	148	162	55

Expression is determined relative to detection of transcripts in vehicle-treated control cells

Table 3: Genes with altered expression after treatment in the “lipid storage state” which are significantly associated with lipid handling pathways.

Treatment	Change	Lipid synthesis	Lipid accumulation	Concentration of lipid
1 μ M Quercetin	up	HMOX1	SPHK1, UCGC, HMOX1	SPHK1, UCGC, NGF, HMGA1, HMOX1
	down	SREBF1, THRSP, PNPL3A, GPAM, ACAC3, PRKD1, LPL1, LPIN1, IGF1, FASN, LTF	SREBF1, SPHK1, IGF1, FASN	SREBF1, THRSP, GPAM, SPHK1, LPL1, LPIN1, IGF1, FASN
1 μ M Ferulic Acid	up	NFATC2, SIPR3, APOC1, CXCL8, SPHK1, UCGC, F2RL1, FOSL1, LIF	HMOX1, SPHK1, UCGC	HMOX1, SPHK1, UCGC
	down	CNTFR	ALDH1L1, DHRS3, FABP4, IGF1	ABCA1, IGF1, LPL, GPAM, THRSP
Combined treatment	up	SIPR3, UGCG, CCL2, CYP1B1, F2RL1, LIF, NFATC2	HMOX1, SPHK1, UGCG	HMOX1, SPHK1, UGCG, HMGA1
	down	APOC1, LTF	ALDH1L1, DHRS3, FABP4, IGF1	ABCA1, IGF1, LPL, ADORA1, GPAM, THRSP

n = 3 for each treatment.

Table 4: The effect of treatment on the mole fraction of lipid species in the “ongoing lipogenesis state”.

Molecular Species	Quercetin	Ferulic Acid	Quercetin + ferulic acid	Affected by differentiation
DAG (12:0/16:0)	N.S	N.S	61.5 *	no
DAG (12:0/18:1)	N.S	N.S	78.6 *	no
DAG (14:0/16:0)	N.S	N.S	79.0 *	yes
DAG (14:0/18:2)	N.S	N.S	76.0 **	no
TAG 42:0-FA 16:0	73.5 *	N.S	73.5 *	yes
TAG 44:0-FA 12:0	N.S	N.S	75.8 *	yes
TAG 44:1-FA 18:0	80.0 *	N.S	N.S	no
TAG 46:0-FA 12:0	N.S	N.S	66.9 *	no
TAG 46:1-FA 12:0	N.S	N.S	80.0 *	no
TAG 50:5-FA 18:2	114.3 *	N.S	N.S	no
TAG 52:3-FA 16:0	120.0 *	N.S	N.S	no
TAG 52:3-FA 18:2	115.6 *	N.S	N.S	no
TAG 52:3-FA 20:2	127.7 **	N.S	N.S	no
TAG 52:3-FA 22:1	N.S	117.6 **	N.S	no
TAG 52:5-FA 18:2	N.S	141.7 *	N.S	no
FFA (14:1)	46.3 *	N.S	N.S	yes
FFA (15:0)	68.4 **	76.9 *	70.5 **	yes
CE (18:4)	154.0 *	162.0 *	N.S	no
PC (16:0/16:0)	127.6 *	N.S	124.6 *	yes
PC (18:0/14:1)	N.S	N.S	18.1 *	no
PE (O-16:0/18:2)	N.S	533.3 *	N.S	no
PE (18:1/22:4)	85.4 *	N.S	N.S	no
HCER (18:1)	N.S	129.4 *	N.S	no
DCER (24:1)	N.S	N.S	112.4 *	yes

The effect of treatment is expressed as a percentage of the vehicle treatment (100%). Mole fraction is the relative amount of a particular species as a percentage of all lipid species of that lipid class. All other detected metabolites (not listed) were not significantly affected in all 3 treatments. n = 5. N.S, not significant. * $p < 0.05$, ** $p < 0.01$, *** $p < 0.001$

Table 5: The effect of treatment on adipocytes in the “ongoing lipogenesis state” on gene expression related to lipid handling pathways.

Treatment	Change	Lipid synthesis	Lipid accumulation	Conversion of lipid
1 μ M quercetin	up	IGFBP4	SPHK1	SPHK1
	down	HMGCR, C3, FDPS, MID1PT	HMGCR, IGF1	HMGCR, IGF1, ADH4
Combined treatment	up	HMOX1, HMGA1	HMOX1	HMOX1
	down	HMGCR, IGF1, CD36	HMGCR, IGF1	HMGCR, ADH4, PTGER3

No changes relevant to lipid handling were seen in cells treated with 1 μ M ferulic acid. n = 3 for each treatment.

FIGURE LEGENDS

Fig. 1: Experimental set up for promotion of differentiation and subsequent treatment of SGBS cells

Maturation of SGBS cells was promoted by changes of media every 4 d with cells receiving their first treatment on day 14 (T = 0 h). Basal medium was DMEM/F-12 medium supplemented with 1% (v/v) penicillin-streptomycin solution, 1% (v/v) pan-bio solution.

Growth phase: Basal medium with 10% (v/v) fetal bovine serum. Adipogenesis phase: Basal medium supplemented with 125 nM transferrin, 20 nM human insulin, 100 nM cortisol, 0.2 nM triiodothyronine (T3), 25 nM dexamethasone, 250 μ M 3-isobutyl-1-methylxanthine and 2 μ M rosiglitazone. Lipogenesis phase: Basal medium supplemented with 125 nM transferrin, 20 nM insulin, 100 nM cortisol and 0.2 nM T3. Treatment phase: At 14 d, cells were treated under two conditions: “ongoing lipogenic state” with basal medium supplemented with 125 nM transferrin, 20 nM insulin, 100 nM cortisol and 0.2 nM T3, or “lipid storage state” with cells in basal medium. Treatments were vehicle (DMSO), quercetin, ferulic acid or a combined quercetin and ferulic acid treatment, at time zero (day = 14 d) and then every 24 h for up to 48 h (Time = 0, 24 and 48 h). At t = 54 h, cells were harvested for transcriptomic analysis, and after t = 72 h, for lipidomic analysis.

Fig. 2: Differentiated SGBS cells display a mature adipocyte phenotype

Differentiation of pre-adipocytes initially promotes morphological changes of SGBS cells (A). Storage of lipid is seen in cells differentiated for 2 weeks or longer (Bi & Bii) and is confirmed as lipid deposits by Oil Red O staining (Biii). Example images shown at each time point. Scale bar represents 200 μ m, and all images are of same magnification. Differentiated SGBS cells (15 d) exhibit significant insulin-sensitive glucose uptake (C). n = 6 for each group. Lipid accumulation significantly increases between day 14 and 17 when

differentiation factors are maintained in culture (“ongoing lipogenesis state), but no significant further lipid deposition is evidenced when differentiation factors are removed from the culture media (“lipid storage state”) (D). $n = 9$ biological replicates for each group. Data expressed as mean \pm SEM. $*p < 0.05$, $**p < 0.01$.

Fig. 3: Treatment does not significantly affect cell number or viability of differentiated SGBS cells.

The number of live SGBS cells (A) and cell viability using trypan blue exclusion (B) were not significantly affected by (poly)phenol treatment (3×24 h treatment). Mean \pm SEM, $n = 5$.

Fig. 4: Quality of transcriptome data for assessing treatment effects on gene expression

The 3 samples selected for analysis of transcript expression show limited batch variation. Samples analysed from 54 h treated vehicle (A541-3) and 54 h $1 \mu\text{M}$ quercetin with $1 \mu\text{M}$ ferulic acid (D541-3) in lipid storage conditions are presented (A). Detection of significantly altered transcripts (in red) is independent of their level of expression and follows a normal distribution. Transcripts from 54 h $1 \mu\text{M}$ quercetin with $1 \mu\text{M}$ ferulic acid relative to transcript expression in 54 h vehicle-treated cells in lipid storage conditions are shown (B). Principal component analysis (PCA) showed that one factor contributes 89% of the total variance when assessing the effect of the combined $1 \mu\text{M}$ quercetin with $1 \mu\text{M}$ ferulic acid treatment (D54, light blue) compared to vehicle treatment (A54, red) for cells treated for 54 h in the “lipid storage state” (C).

Fig. 5: Changes in the mole fraction of lipid species in SGBS cells in the “ongoing lipogenic state” relative to the “lipid storage state”

Only changes are shown where the level of each individual lipid species was significantly different ($p < 0.05$) in the “ongoing lipogenic state” compared to the “lipid storage state”; ** $p < 0.01$; * = $p < 0.05$). The abundance of a lipid species is expressed relative to all lipids in that class and is expressed as species fold change (from 1.0) within the respective lipid class. No significant effect ($p > 0.05$) of ongoing lipogenesis was detected for changes in total lipid class, expressed as fold change of total lipids detected, shown in the column on the right-hand side. Magnitude of changes are proportional to colour intensity of the bars; increased fold change shown as red bar or highlight and decreased fold change as blue bar or highlight. $n = 5$ independent experiments.

Fig. 6: Effect of treatment on neutral intracellular lipid deposits in the “lipid storage state”

1 μM quercetin, 1 μM ferulic acid or a combined treatment, each for three sequential 24 h doses, significantly reduces lipid deposits from differentiated SGBS cells cultured in lipid storing conditions (A). $n \geq 9$ biological replicates for each treatment. No significant effects of two 24 h (poly)phenol treatments (B) ($n = 8$ biological replicates for each group) or one 72 h treatment (C) ($n = 9$ biological replicates for each group) were found on stored lipid. V = vehicle, Q = quercetin, Fr A = ferulic acid. Data shown as mean \pm SEM. * $p < 0.05$, ** $p < 0.01$, *** $p < 0.001$.

Fig. 7: Chronic (poly)phenol treatment in the “lipid storage state” drives changes in gene expression related to lipid handling via PPAR/RXR signalling

(A) The number of individual transcripts modified by 3×24 h (poly)phenol (1 μM of each) treatments. (B) Gene changes associated with (poly)phenol treatments are significantly ($P < 0.001$, threshold line) related to lipid handling systems and metabolic conditions. For each

category, top bar = 1 μ M quercetin, middle bar = 1 μ M ferulic acid and lower bar = quercetin + ferulic acid (1 μ M each).

Relationship predicted by IPA showing how quercetin (C), ferulic acid (D) and quercetin + ferulic acid (E) treatment (1 μ M each) impact on lipid handling in the “lipid storage state”. Red and green fill show increased and decreased gene expression respectively. The predicted effect of altered gene expression on lipid handling is shown by blue (inhibition), orange (activation), grey (undetermined) or yellow (inconsistent with obtained data) arrows. The predicted effects of canonical pathway signalling (CP), PPAR α /RXR α , on the gene changes detected in chronic quercetin (F), ferulic acid (G) and combined (H) treated SGBS cells. Pink highlighted genes are strongly related to lipid handling. Other colour coding as for C-E. n = 3 biological replicates; **a** = lipid accumulation; **b** = lipid synthesis; **c** = lipid concentration.

Fig. 8: Neutral lipid accumulation is attenuated by combined (poly)phenol treatment at a higher concentration during the “ongoing lipogenic state”.

Chronic treatment (3 \times 24 h doses) with 1 μ M (poly)phenol has no significant effect on lipid accumulation during ongoing lipogenesis (A.) n \geq 9 biological replicates for each treatment. Combined 10 μ M quercetin and 10 μ M ferulic acid chronic treatment, but not individual 10 μ M treatments, significantly attenuates lipid accumulation during the promotion of ongoing lipogenesis SGBS cells (B.) n = 9 biological replicates for each treatment. V = vehicle, Q = quercetin, Fr A = ferulic acid. Data shown as mean \pm SEM. ***P* < 0.01.

Fig. 9: Chronic (poly)phenol treatment during the “ongoing lipogenic state”

The number of individual transcripts can be modified by one or multiple chronic (poly)phenol treatments (A). Gene changes associated with (poly)phenol treatments are significantly (*p* < 0.001, orange threshold line) related to lipid handling systems and

metabolic conditions (B). For each system, the top bar represents 1 μ M quercetin, middle bar represents 1 μ M ferulic acid and lower bar represents quercetin + ferulic acid treatment. Panel C and D show genes altered by quercetin and quercetin and ferulic acid treatment respectively are predicted to impact on lipid handling. Red and green fill show increased and decreased gene expression respectively. The predicted effect of altered gene expression on lipid handling is shown by blue (inhibition), orange (activation), grey (undetermined) or yellow (inconsistent with obtained data) arrows. n = 3 biological replicates; **a** = lipid accumulation; **b** = lipid synthesis; **c** = lipid concentration.

FIGURES

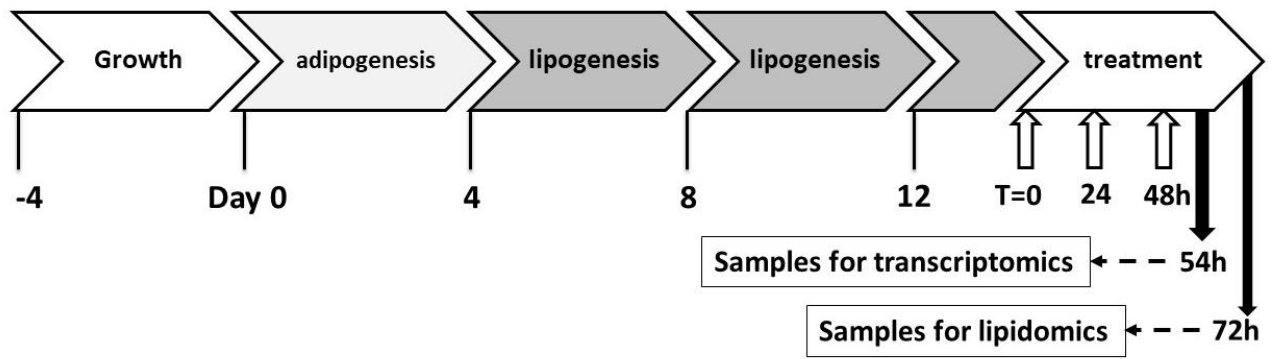


Fig. 1

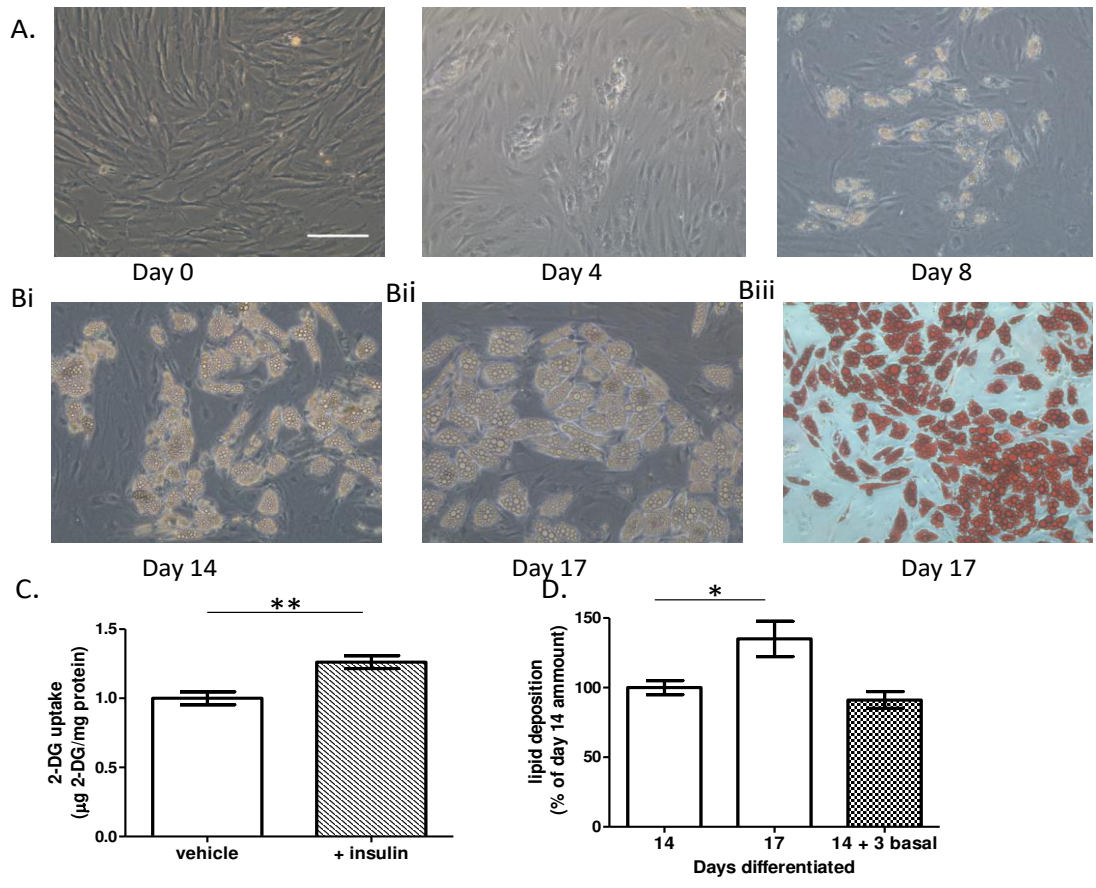


Fig. 2

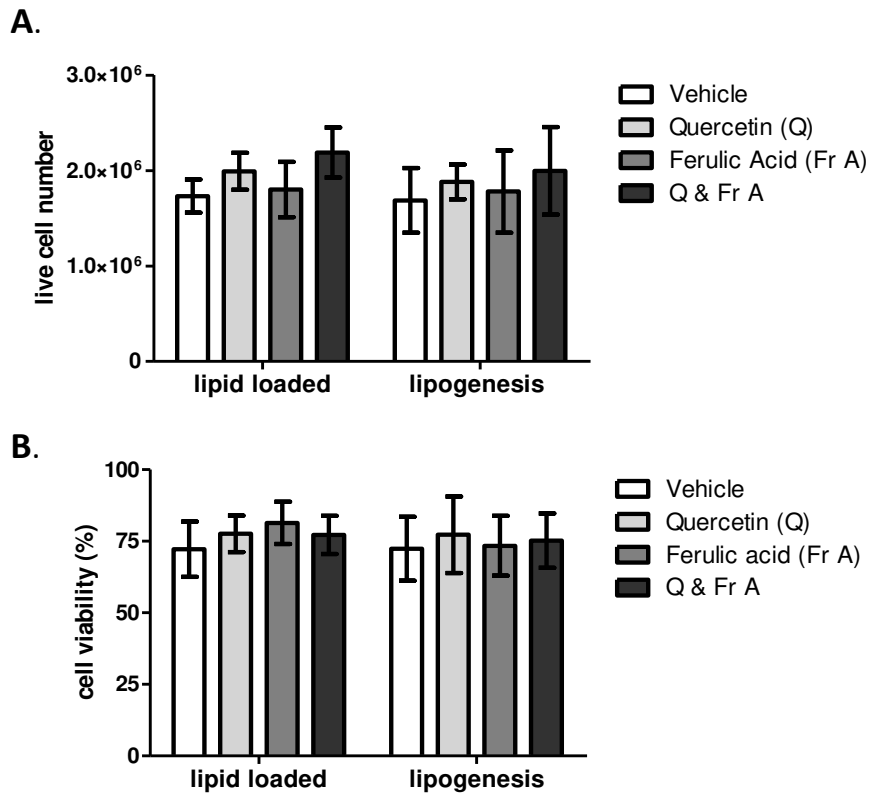


Fig. 3

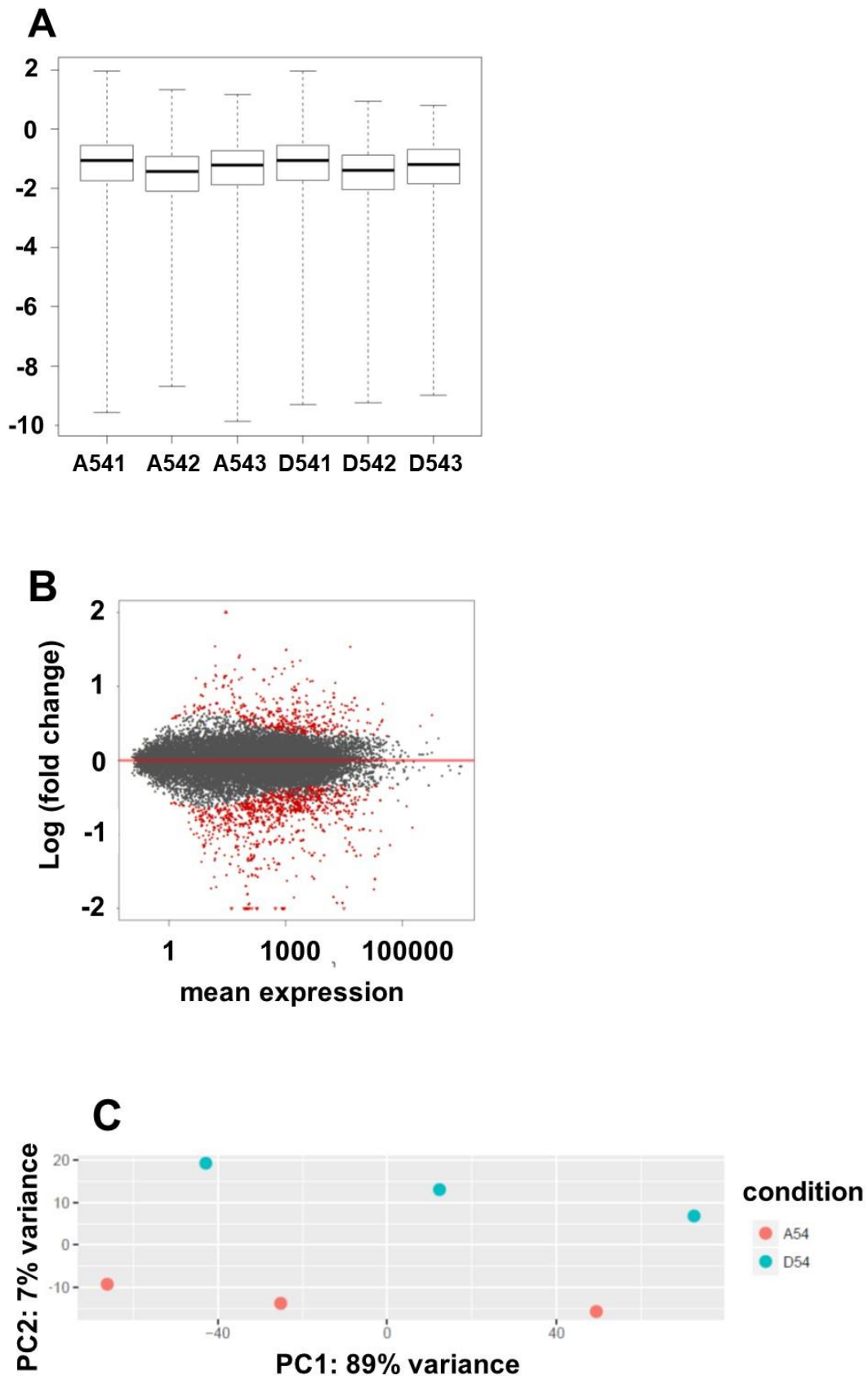


Fig. 4



Fig. 5

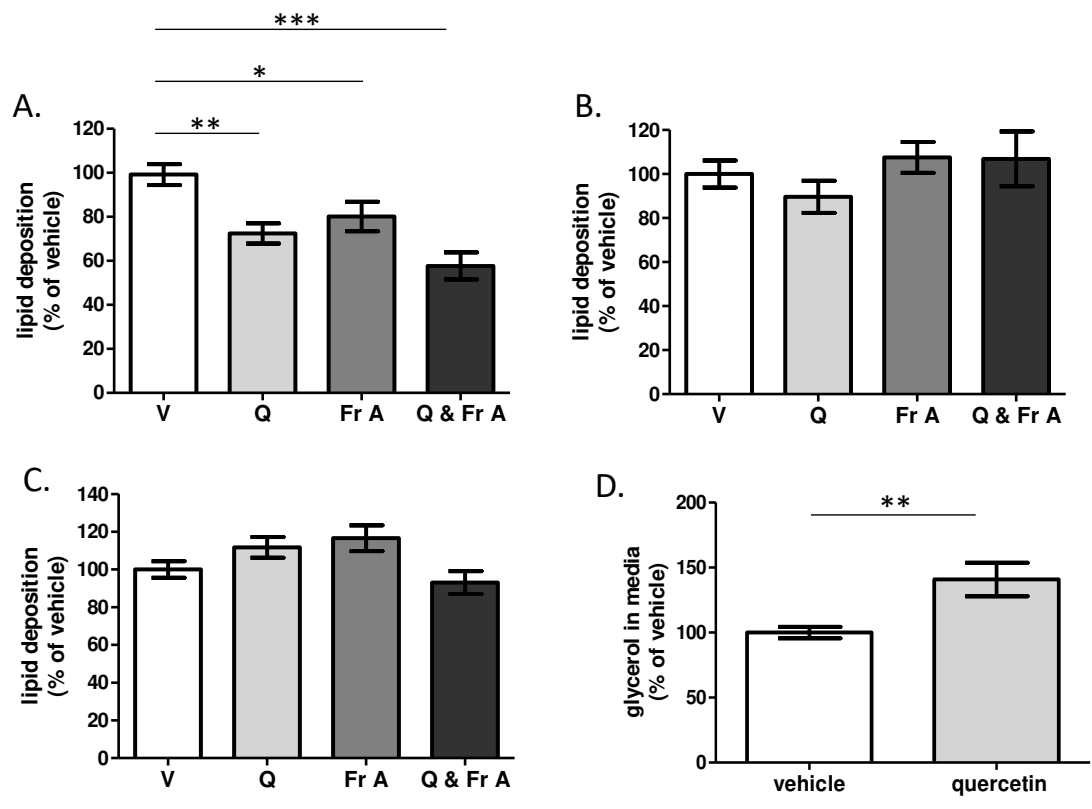


Fig. 6

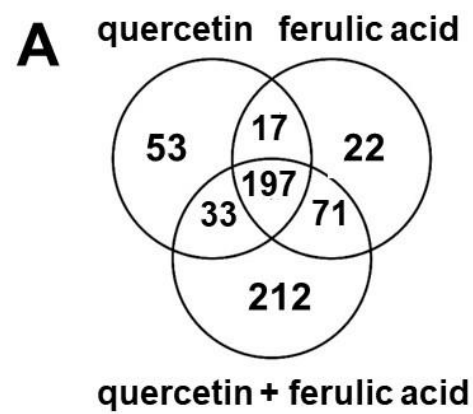


Fig. 7A

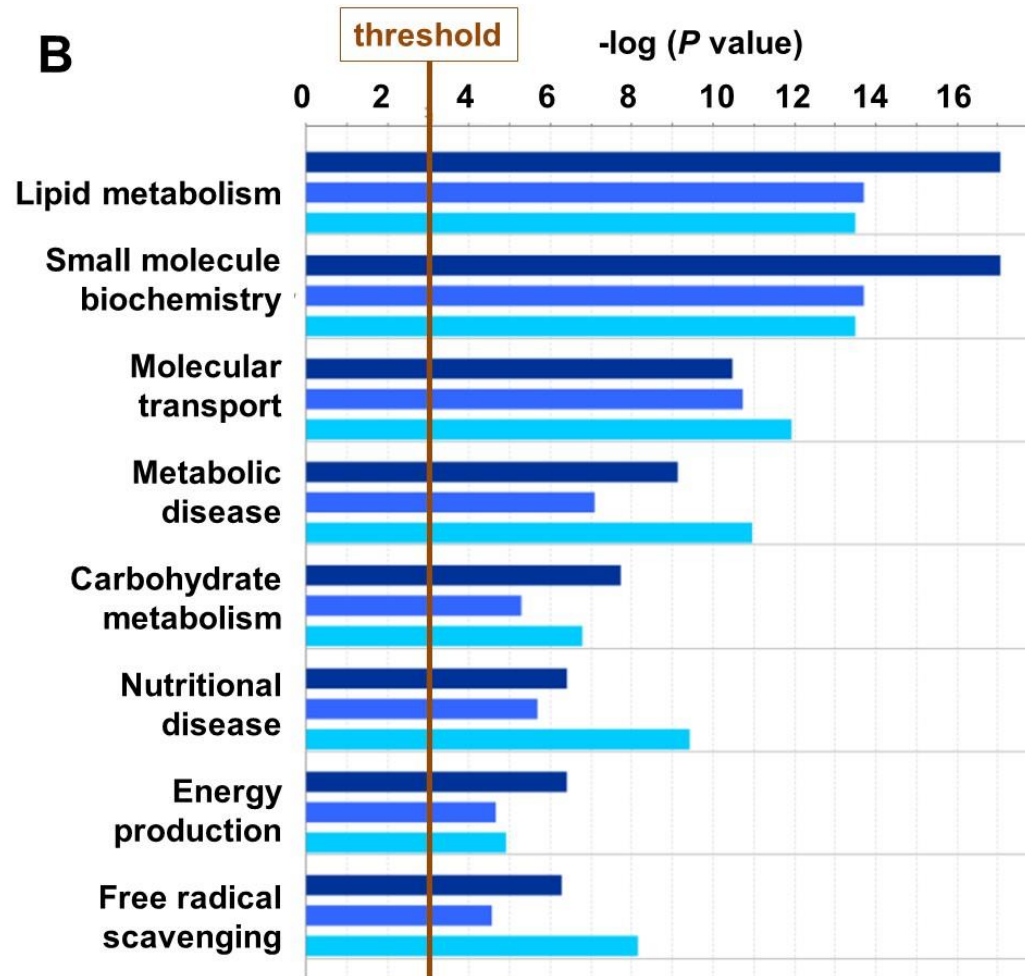
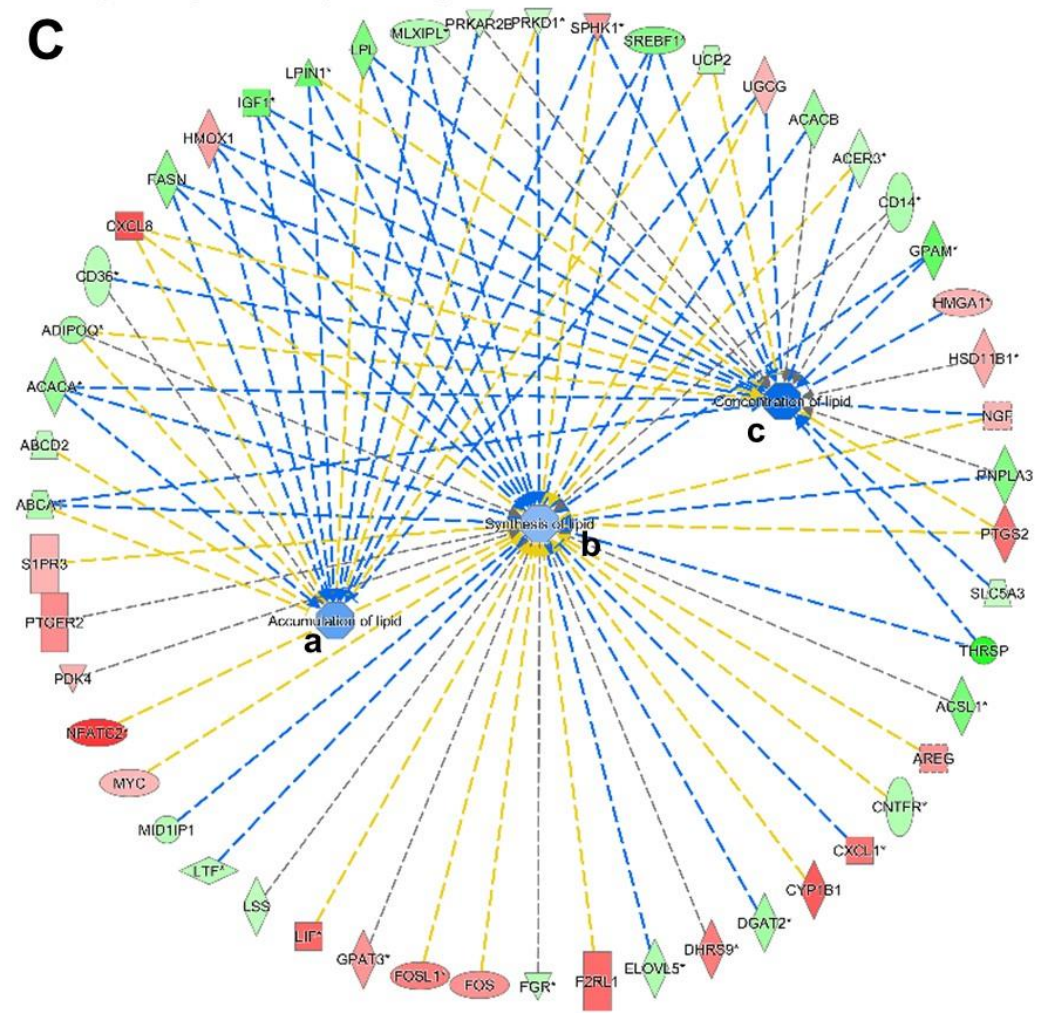


Fig. 7B

C**Fig. 7C**

D

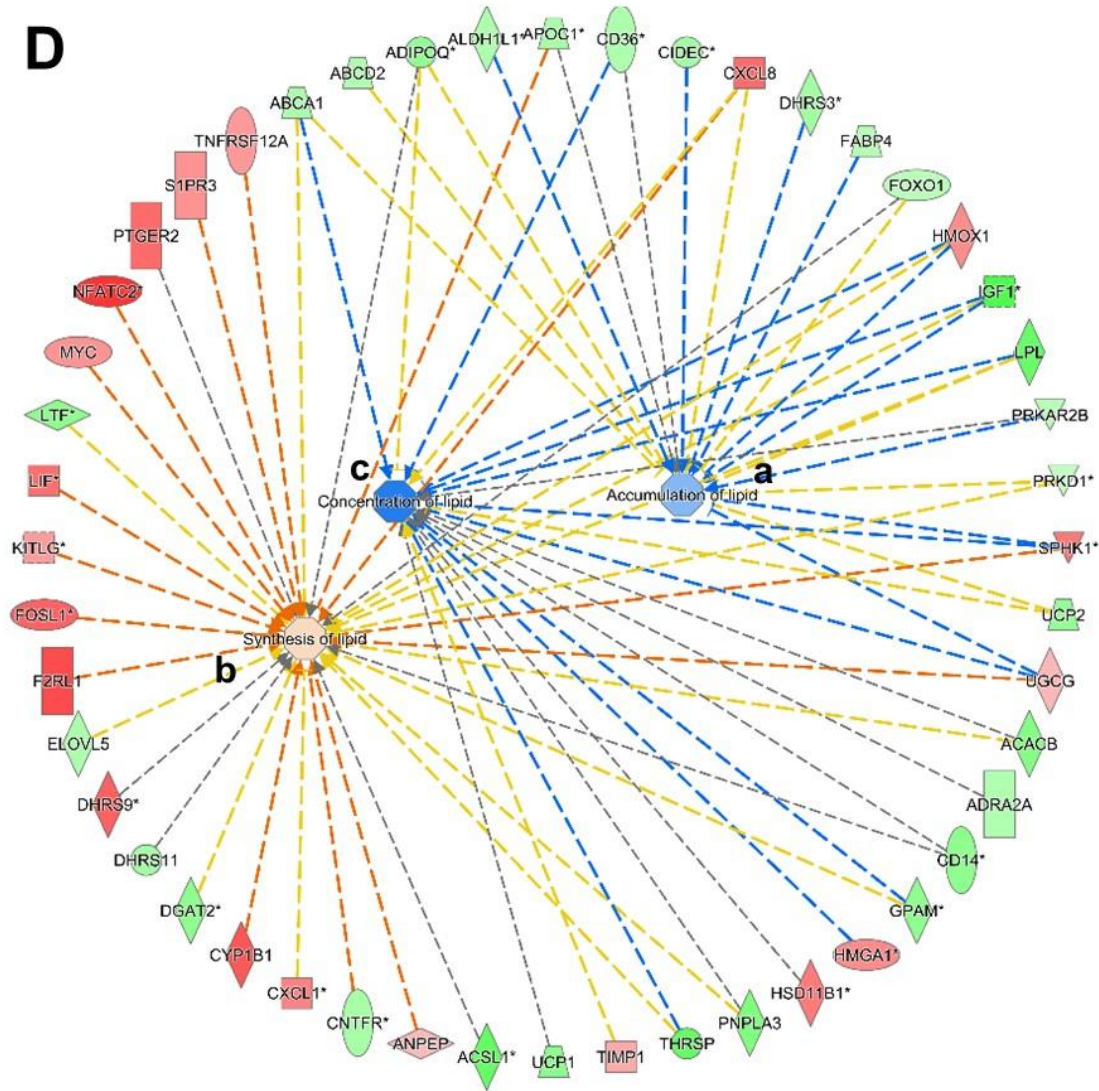


Fig. 7D

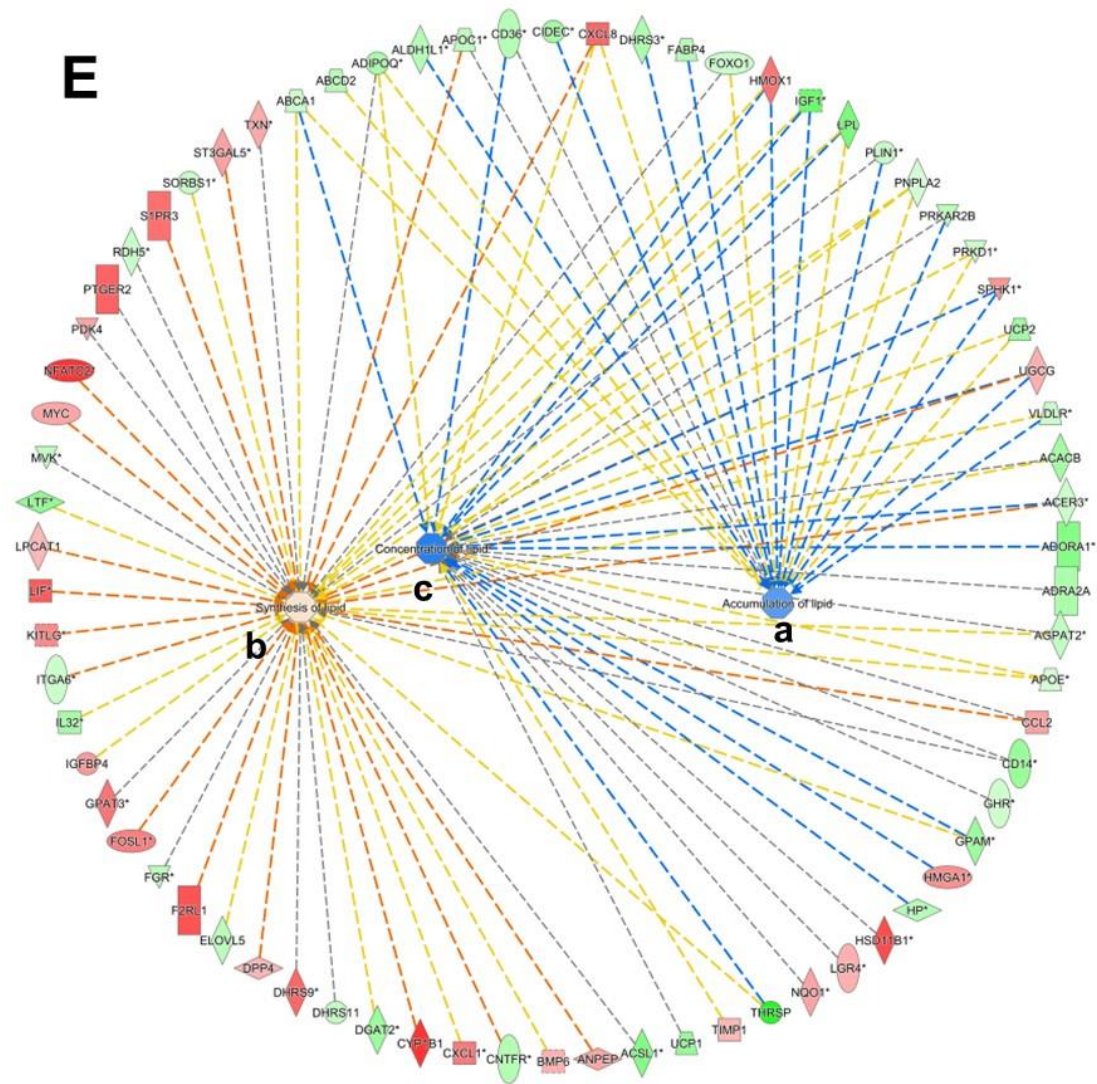


Fig. 7E

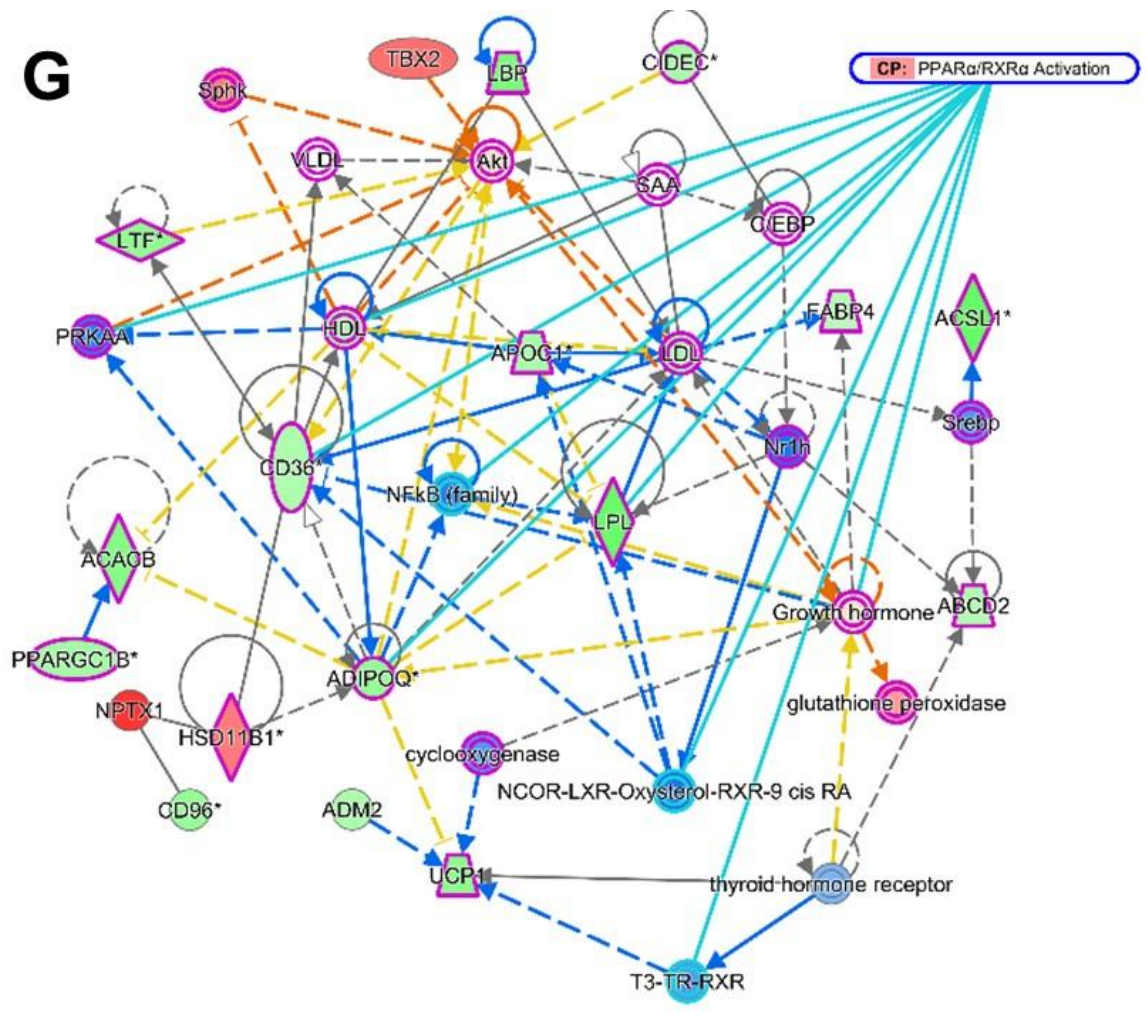


Fig. 7G

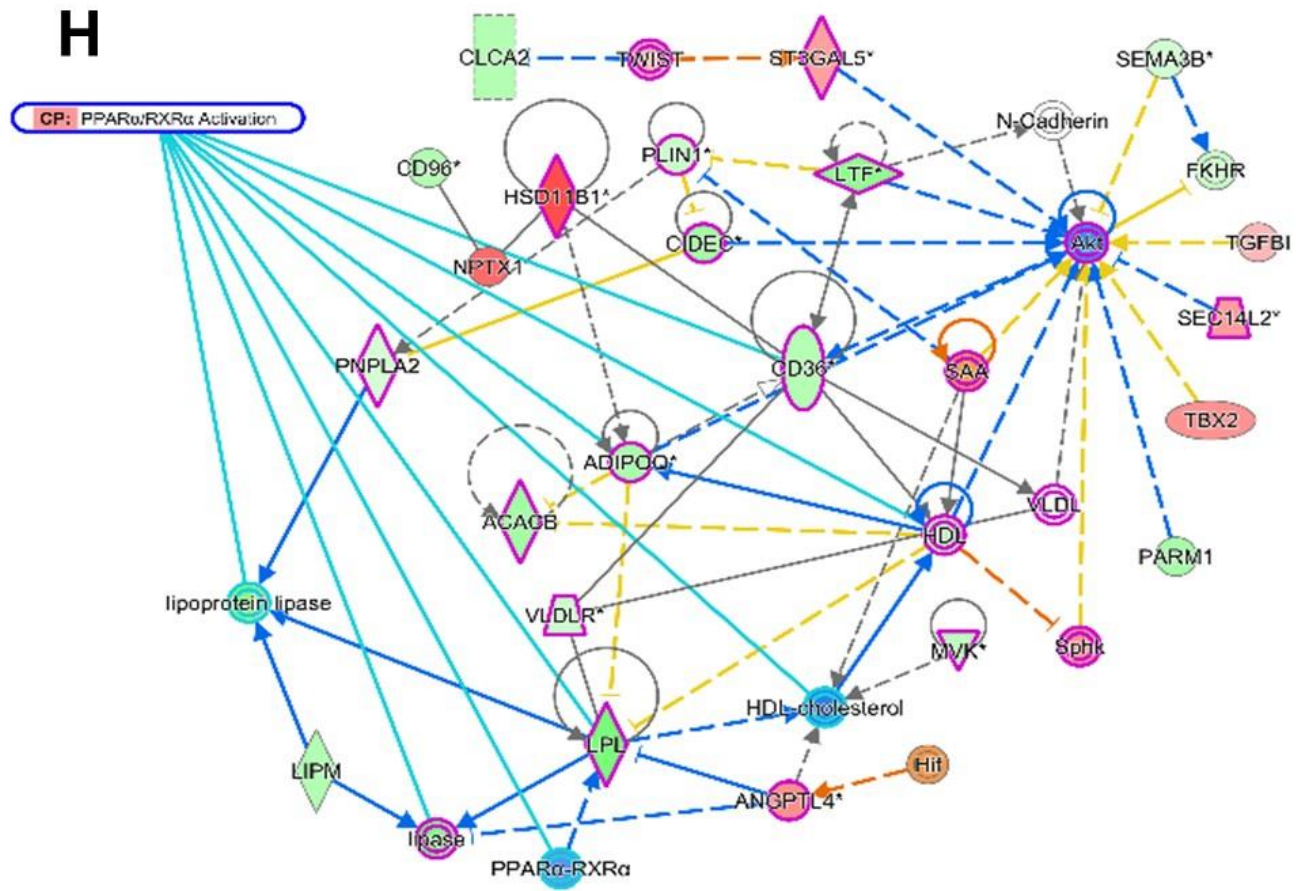


Fig. 7H

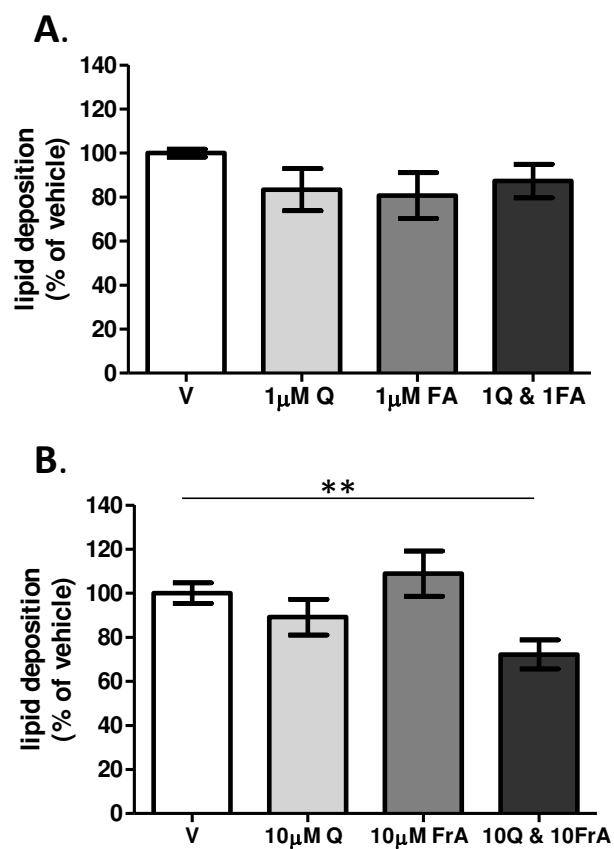


Fig. 8

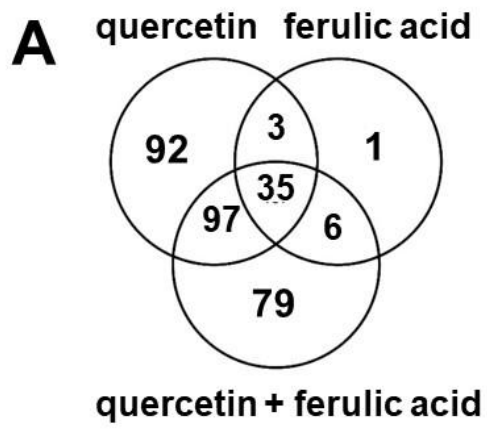


Fig. 9A

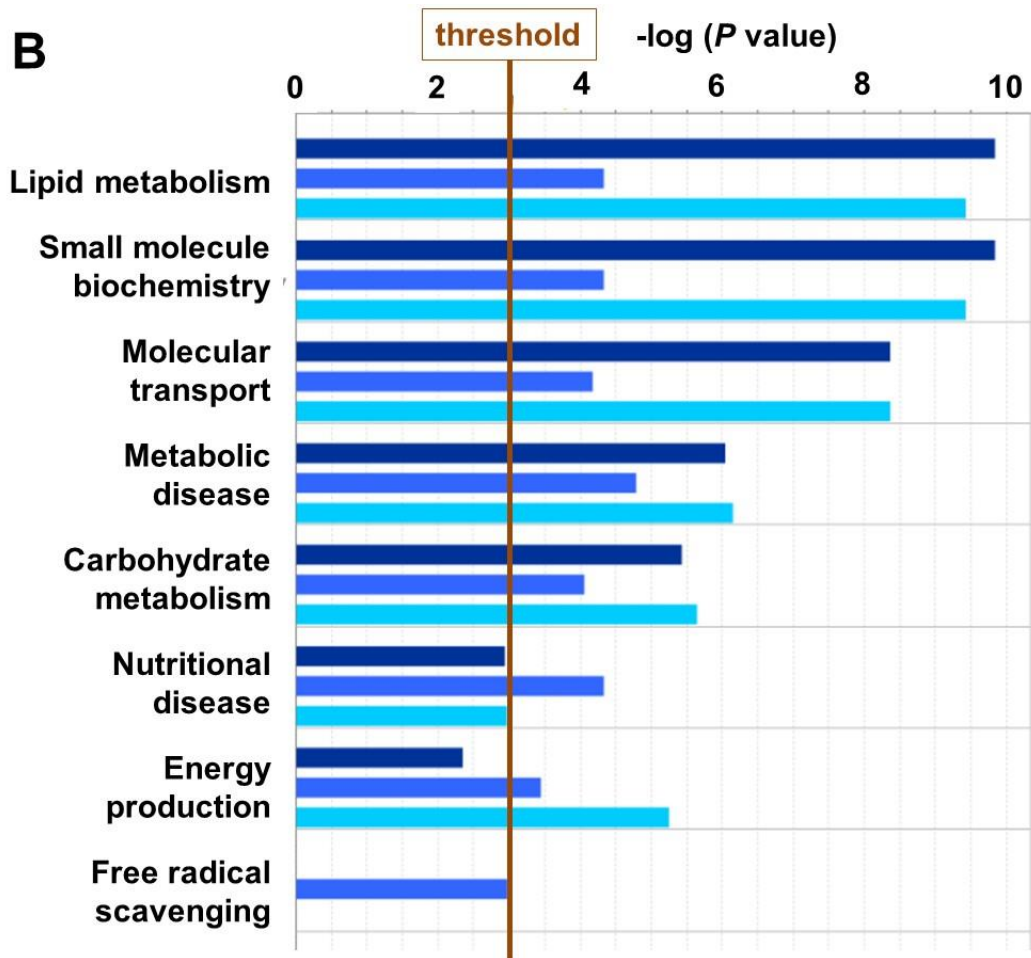


Fig. 9B

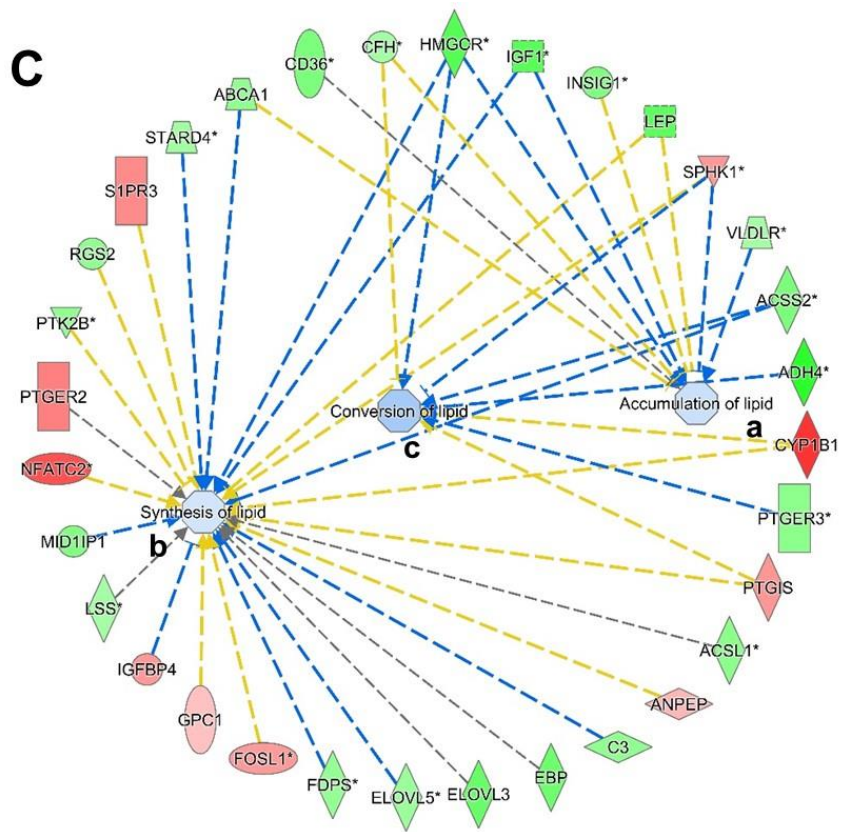


Fig. 9C

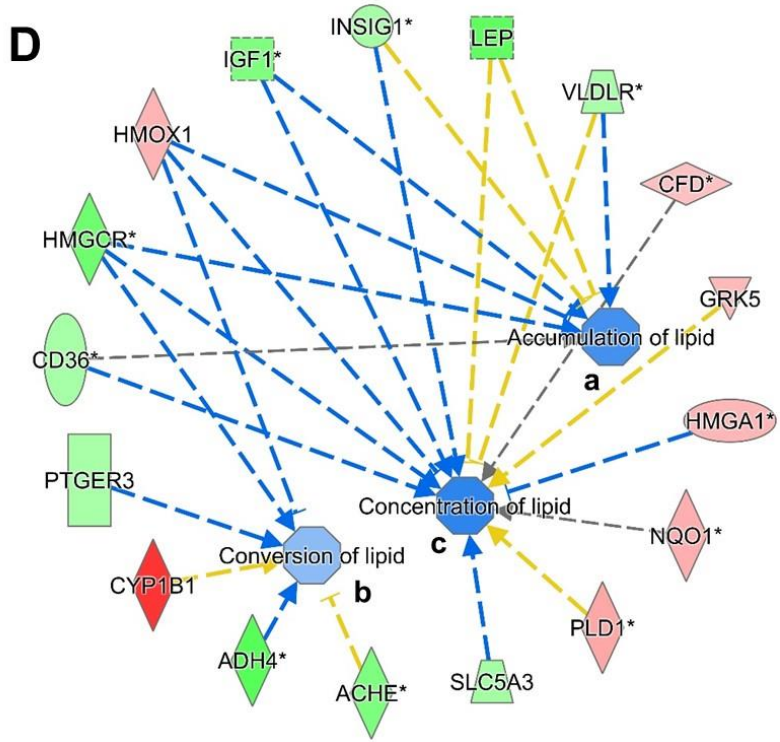


Fig. 9D

REFERENCES

1. Rajala, M. W., and P. E. Scherer. 2003. Minireview: The adipocyte--at the crossroads of energy homeostasis, inflammation, and atherosclerosis. *Endocrinology* **144**: 3765-3773.
2. Bastien, M., P. Poirier, I. Lemieux, and J. P. Despres. 2014. Overview of epidemiology and contribution of obesity to cardiovascular disease. *Prog Cardiovasc Dis* **56**: 369-381.
3. Ting, Y., W. T. Chang, D. K. Shiau, P. H. Chou, M. F. Wu, and C. L. Hsu. 2018. Antiobesity Efficacy of Quercetin-Rich Supplement on Diet-Induced Obese Rats: Effects on Body Composition, Serum Lipid Profile, and Gene Expression. *J Agric Food Chem* **66**: 70-80.
4. Zhao, L., Q. Zhang, W. Ma, F. Tian, H. Shen, and M. Zhou. 2017. A combination of quercetin and resveratrol reduces obesity in high-fat diet-fed rats by modulation of gut microbiota. *Food Funct* **8**: 4644-4656.
5. Hoek-van den Hil, E. F., E. M. van Schothorst, I. van der Stelt, H. J. Swarts, M. van Vliet, T. Amolo, J. J. Vervoort, D. Venema, P. C. Hollman, I. M. Rietjens, and J. Keijer. 2015. Direct comparison of metabolic health effects of the flavonoids quercetin, hesperetin, epicatechin, apigenin and anthocyanins in high-fat-diet-fed mice. *Genes Nutr* **10**: 469.
6. Kobori, M., S. Masumoto, Y. Akimoto, and Y. Takahashi. 2009. Dietary quercetin alleviates diabetic symptoms and reduces streptozotocin-induced disturbance of hepatic gene expression in mice. *Mol Nutr Food Res* **53**: 859-868.
7. de Melo, T. S., P. R. Lima, K. M. Carvalho, T. M. Fontenele, F. R. Solon, A. R. Tome, T. L. de Lemos, S. G. da Cruz Fonseca, F. A. Santos, V. S. Rao, and M. G. de

Queiroz. 2017. Ferulic acid lowers body weight and visceral fat accumulation via modulation of enzymatic, hormonal and inflammatory changes in a mouse model of high-fat diet-induced obesity. *Braz J Med Biol Res* **50**: e5630.

8. Naowaboot, J., P. Piyabhan, N. Munkong, W. Parklak, and P. Pannangpetch. 2016. Ferulic acid improves lipid and glucose homeostasis in high-fat diet-induced obese mice. *Clin Exp Pharmacol Physiol* **43**: 242-250.

9. Frank, J., N. K. Fukagawa, A. R. Bilia, E. J. Johnson, O. Kwon, V. Prakash, T. Miyazawa, M. N. Clifford, C. D. Kay, A. Crozier, J. W. Erdman, A. Shao, and G. Williamson. 2019. Terms and nomenclature used for plant-derived components in nutrition and related research: efforts toward harmonization. *Nutr Rev*: nuz081.

10. Guo, X., J. Liu, S. Cai, O. Wang, and B. Ji. 2016. Synergistic interactions of apigenin, naringin, quercetin and emodin on inhibition of 3T3-L1 preadipocyte differentiation and pancreas lipase activity. *Obes Res Clin Pract* **10**: 327-339.

11. Seo, Y. S., O. H. Kang, S. B. Kim, S. H. Mun, D. H. Kang, D. W. Yang, J. G. Choi, Y. M. Lee, D. K. Kang, H. S. Lee, and D. Y. Kwon. 2015. Quercetin prevents adipogenesis by regulation of transcriptional factors and lipases in OP9 cells. *Int J Mol Med* **35**: 1779-1785.

12. Bae, C. R., Y. K. Park, and Y. S. Cha. 2014. Quercetin-rich onion peel extract suppresses adipogenesis by down-regulating adipogenic transcription factors and gene expression in 3T3-L1 adipocytes. *J Sci Food Agric* **94**: 2655-2660.

13. Mosqueda-Solis, A., A. Lasa, S. Gomez-Zorita, I. Eseberri, C. Pico, and M. P. Portillo. 2017. Screening of potential anti-adipogenic effects of phenolic compounds showing different chemical structure in 3T3-L1 preadipocytes. *Food Funct* **8**: 3576-3586.

14. Leiherer, A., K. Stoemmer, A. Muendlein, C. H. Saely, E. Kinz, E. M. Brandtner, P. Fraunberger, and H. Drexel. 2016. Quercetin Impacts Expression of Metabolism- and Obesity-Associated Genes in SGBS Adipocytes. *Nutrients* **8**.
15. Seo, M.-J., Y.-J. Lee, J.-H. Hwang, K.-J. Kim, and B.-Y. Lee. 2015. The inhibitory effects of quercetin on obesity and obesity-induced inflammation by regulation of MAPK signaling. *J Nutr Biochem* **26**: 1308-1316.
16. Koh, E.-J., K.-J. Kim, Y.-J. Seo, J. Choi, and B.-Y. Lee. 2017. Modulation of HO-1 by Ferulic Acid Attenuates Adipocyte Differentiation in 3T3-L1 Cells. *Molecules* **22**: 745.
17. Wabitsch, M., R. E. Brenner, I. Melzner, M. Braun, P. Moller, E. Heinze, K. M. Debatin, and H. Hauner. 2001. Characterization of a human preadipocyte cell strain with high capacity for adipose differentiation. *Int J Obes Relat Metab Disord* **25**: 8-15.
18. Fischer-Posovszky, P., F. S. Newell, M. Wabitsch, and H. E. Tornqvist. 2008. Human SGBS cells - a unique tool for studies of human fat cell biology. *Obes Facts* **1**: 184-189.
19. Guennoun, A., M. Kazantzis, R. Thomas, M. Wabitsch, D. Tews, K. Seetharama Sastry, M. Abdelkarim, V. Zilberfarb, A. D. Strosberg, and L. Chouchane. 2015. Comprehensive molecular characterization of human adipocytes reveals a transient brown phenotype. *J Transl Med* **13**: 135.
20. Martin, M. 2011. Cutadapt removes adapter sequences from high-throughput sequencing reads. *2011* **17**: 3.
21. Dobin, A., C. A. Davis, F. Schlesinger, J. Drenkow, C. Zaleski, S. Jha, P. Batut, M. Chaisson, and T. R. Gingeras. 2013. STAR: ultrafast universal RNA-seq aligner. *Bioinformatics* **29**: 15-21.

22. O'Leary, N. A., M. W. Wright, J. R. Brister, S. Ciuffo, D. Haddad, R. McVeigh, B. Rajput, B. Robbertse, B. Smith-White, D. Ako-Adjei, A. Astashyn, A. Badretdin, Y. Bao, O. Blinkova, V. Brover, V. Chetvernin, J. Choi, E. Cox, O. Ermolaeva, C. M. Farrell, T. Goldfarb, T. Gupta, D. Haft, E. Hatcher, W. Hlavina, V. S. Joardar, V. K. Kodali, W. Li, D. Maglott, P. Masterson, K. M. McGarvey, M. R. Murphy, K. O'Neill, S. Pujar, S. H. Rangwala, D. Rausch, L. D. Riddick, C. Schoch, A. Shkeda, S. S. Storz, H. Sun, F. Thibaud-Nissen, I. Tolstoy, R. E. Tully, A. R. Vatsan, C. Wallin, D. Webb, W. Wu, M. J. Landrum, A. Kimchi, T. Tatusova, M. DiCuccio, P. Kitts, T. D. Murphy, and K. D. Pruitt. 2016. Reference sequence (RefSeq) database at NCBI: current status, taxonomic expansion, and functional annotation. *Nucleic Acids Res* **44**: D733-D745.
23. Kent, W. J., C. W. Sugnet, T. S. Furey, K. M. Roskin, T. H. Pringle, A. M. Zahler, and D. Haussler. 2002. The human genome browser at UCSC. *Genome Res* **12**: 996-1006.
24. Li, H., B. Handsaker, A. Wysoker, T. Fennell, J. Ruan, N. Homer, G. Marth, G. Abecasis, R. Durbin, and S. Genome Project Data Processing. 2009. The Sequence Alignment/Map format and SAMtools. *Bioinformatics* **25**: 2078-2079.
25. McKenna, A., M. Hanna, E. Banks, A. Sivachenko, K. Cibulskis, A. Kernysky, K. Garimella, D. Altshuler, S. Gabriel, M. Daly, and M. A. DePristo. 2010. The Genome Analysis Toolkit: a MapReduce framework for analyzing next-generation DNA sequencing data. *Genome Res* **20**: 1297-1303.
26. Okonechnikov, K., A. Conesa, and F. García-Alcalde. 2016. Qualimap 2: advanced multi-sample quality control for high-throughput sequencing data. *Bioinformatics* **32**: 292-294.

27. Liao, Y., G. K. Smyth, and W. Shi. 2014. featureCounts: an efficient general purpose program for assigning sequence reads to genomic features. *Bioinformatics* **30**: 923-930.
28. Love, M. I., W. Huber, and S. Anders. 2014. Moderated estimation of fold change and dispersion for RNA-seq data with DESeq2. *Genome Biol* **15**: 550-550.
29. <https://www.qiagenbioinformatics.com/products/ingenuity-pathway-analysis/>. 2019. Ingenuity Pathway Analysis. QIAGEN Inc.
30. Kramer, A., J. Green, J. Pollard, Jr., and S. Tugendreich. 2014. Causal analysis approaches in Ingenuity Pathway Analysis. *Bioinformatics* **30**: 523-530.
31. Lapid, K., and J. M. Graff. 2017. Form(ul)ation of adipocytes by lipids. *Adipocyte* **6**: 176-186.
32. Chew, W. S., F. Torta, S. Ji, H. Choi, H. Begum, X. Sim, C. M. Khoo, E. Y. H. Khoo, W.-Y. Ong, R. M. Van Dam, M. R. Wenk, E. S. Tai, and D. R. Herr. 2019. Large-scale lipidomics identifies associations between plasma sphingolipids and T2DM incidence. *JCI Insight* **5**: e126925.
33. Apostolopoulou, M., R. Gordillo, C. Koliaki, S. Gancheva, T. Jelenik, E. De Filippo, C. Herder, D. Markgraf, F. Jankowiak, I. Esposito, M. Schlensak, P. E. Scherer, and M. Roden. 2018. Specific Hepatic Sphingolipids Relate to Insulin Resistance, Oxidative Stress, and Inflammation in Nonalcoholic Steatohepatitis. *Diabetes Care* **41**: 1235-1243.
34. Chavez, J. A., M. M. Siddique, S. T. Wang, J. Ching, J. A. Shayman, and S. A. Summers. 2014. Ceramides and glucosylceramides are independent antagonists of insulin signaling. *J Biol Chem* **289**: 723-734.

35. Hummasti, S., and P. Tontonoz. 2006. The peroxisome proliferator-activated receptor N-terminal domain controls isotype-selective gene expression and adipogenesis. *Mol Endocrinol* **20**: 1261-1275.
36. Toedebusch, R. G., M. D. Roberts, K. D. Wells, J. M. Company, K. M. Kanosky, J. Padilla, N. T. Jenkins, J. W. Perfield, 2nd, J. A. Ibdah, F. W. Booth, and R. S. Rector. 2014. Unique transcriptomic signature of omental adipose tissue in Ossabaw swine: a model of childhood obesity. *Physiol Genomics* **46**: 362-375.
37. Kawakami, K., T. Onaka, M. Iwase, I. Homma, and K. Ikeda. 2005. Hyperphagia and obesity in Na,K-ATPase alpha2 subunit-defective mice. *Obes Res* **13**: 1661-1671.
38. Sidibeh, C. O., M. J. Pereira, X. M. Abalo, G. J Boersma, S. Skrtic, P. Lundkvist, P. Katsogiannos, F. Hausch, C. Castillejo-López, and J. W. Eriksson. 2018. FKBP5 expression in human adipose tissue: potential role in glucose and lipid metabolism, adipogenesis and type 2 diabetes. *Endocrine* **62**: 116-128.
39. Matesanz, N., E. Bernardo, R. Acín-Pérez, E. Manieri, S. Pérez-Sieira, L. Hernández-Cosido, V. Montalvo-Romeral, A. Mora, E. Rodríguez, L. Leiva-Vega, A. V. Lechuga-Vieco, J. Ruiz-Cabello, J. L. Torres, M. Crespo-Ruiz, F. Centeno, C. V. Álvarez, M. Marcos, J. A. Enríquez, R. Nogueiras, and G. Sabio. 2017. MKK6 controls T3-mediated browning of white adipose tissue. *Nat Commun* **8**: 856-856.
40. Take, K., T. Mochida, T. Maki, Y. Satomi, M. Hirayama, M. Nakakariya, N. Amano, R. Adachi, K. Sato, T. Kitazaki, and S. Takekawa. 2016. Pharmacological Inhibition of Monoacylglycerol O-Acyltransferase 2 Improves Hyperlipidemia, Obesity, and Diabetes by Change in Intestinal Fat Utilization. *PLOS ONE* **11**: e0150976.

41. Ota, K., A. Komuro, H. Amano, A. Kanai, K. Ge, T. Ueda, and H. Okada. 2019. High Fat Diet Triggers a Reduction in Body Fat Mass in Female Mice Deficient for Utx demethylase. *Sci Rep* **9**: 10036-10036.
42. Elam, M. B., G. S. Cowan, Jr., R. J. Rooney, M. L. Hiler, C. R. Yellaturu, X. Deng, G. E. Howell, E. A. Park, I. C. Gerling, D. Patel, J. C. Corton, L. M. Cagen, H. G. Wilcox, M. Gandhi, M. H. Bahr, M. C. Allan, L. A. Wodi, G. A. Cook, T. A. Hughes, and R. Raghoebar. 2009. Hepatic gene expression in morbidly obese women: implications for disease susceptibility. *Obesity (Silver Spring)* **17**: 1563-1573.
43. Iqbal, J., M. T. Walsh, S. M. Hammad, M. Cuchel, D. J. Rader, and M. M. Hussain. 2018. ATP binding cassette family A protein 1 determines hexosylceramide and sphingomyelin levels in human and mouse plasma. *J Lipid Res* **59**: 2084-2097.
44. Cuffe, H., M. Liu, C.-C. C. Key, E. Boudyguina, J. K. Sawyer, A. Weckerle, A. Bashore, S. K. Fried, S. Chung, and J. S. Parks. 2018. Targeted Deletion of Adipocyte Abca1 (ATP-Binding Cassette Transporter A1) Impairs Diet-Induced Obesity. *Arterioscler Thromb Vasc Biol* **38**: 733-743.
45. Yang, T. T. C., H. Y. Suk, X. Yang, O. Olabisi, R. Y. L. Yu, J. Durand, L. A. Jelicks, J.-Y. Kim, P. E. Scherer, Y. Wang, Y. Feng, L. Rossetti, I. A. Graef, G. R. Crabtree, and C.-W. Chow. 2006. Role of transcription factor NFAT in glucose and insulin homeostasis. *Mol Cell Biol* **26**: 7372-7387.
46. Schmitz, G., and T. Langmann. 2001. Structure, function and regulation of the ABC1 gene product. *Curr Opin Lipidol* **12**: 129-140.
47. Iankova, I., R. K. Petersen, J. S. Annicotte, C. Chavey, J. B. Hansen, I. Kratchmarova, D. Sarruf, M. Benkirane, K. Kristiansen, and L. Fajas. 2006. Peroxisome proliferator-

activated receptor gamma recruits the positive transcription elongation factor b complex to activate transcription and promote adipogenesis. *Mol Endocrinol* **20**: 1494-1505.

48. Savage, D. B. 2005. PPAR gamma as a metabolic regulator: insights from genomics and pharmacology. *Expert Rev Mol Med* **7**: 1-16.

49. Goldberg, I. J., R. H. Eckel, and N. A. Abumrad. 2009. Regulation of fatty acid uptake into tissues: lipoprotein lipase- and CD36-mediated pathways. *J Lipid Res* **50 Suppl**: S86-S90.

50. Wang, H., L. A. Knaub, D. R. Jensen, D. Young Jung, E. G. Hong, H. J. Ko, A. M. Coates, I. J. Goldberg, B. A. de la Houssaye, R. C. Janssen, C. E. McCurdy, S. M. Rahman, C. Soo Choi, G. I. Shulman, J. K. Kim, J. E. Friedman, and R. H. Eckel. 2009. Skeletal muscle-specific deletion of lipoprotein lipase enhances insulin signaling in skeletal muscle but causes insulin resistance in liver and other tissues. *Diabetes* **58**: 116-124.

51. Pepino, M. Y., L. Love-Gregory, S. Klein, and N. A. Abumrad. 2012. The fatty acid translocase gene CD36 and lingual lipase influence oral sensitivity to fat in obese subjects. *J Lipid Res* **53**: 561-566.

52. Monika, P., and A. Geetha. 2015. The modulating effect of *Persea americana* fruit extract on the level of expression of fatty acid synthase complex, lipoprotein lipase, fibroblast growth factor-21 and leptin--A biochemical study in rats subjected to experimental hyperlipidemia and obesity. *Phytomedicine* **22**: 939-945.

53. Su, J., W. Wu, S. Huang, R. Xue, Y. Wang, Y. Wan, L. Zhang, L. Qin, Q. Zhang, X. Zhu, Z. Zhang, H. Ye, X. Wu, and Y. Li. 2017. PKA-RIIB Deficiency Induces Brown Fatlike Adipocytes in Inguinal WAT and Promotes Energy Expenditure in Male FVB/NJ Mice. *Endocrinology* **158**: 578-591.

54. Grzybek, M., A. Palladini, V. I. Alexaki, M. A. Surma, K. Simons, T. Chavakis, C. Klöse, and Ü. Coskun. 2019. Comprehensive and quantitative analysis of white and brown adipose tissue by shotgun lipidomics. *Molecular Metabolism* **22**: 12-20.
55. Chaurasia, B., V. A. Kaddai, G. I. Lancaster, D. C. Henstridge, S. Sriram, D. L. A. Galam, V. Gopalan, K. N. B. Prakash, S. S. Velan, S. Bulchand, T. J. Tsong, M. Wang, M. M. Siddique, G. Yuguang, K. Sigmundsson, N. A. Mellet, J. M. Weir, P. J. Meikle, M. S. Bin M Yassin, A. Shabbir, J. A. Shayman, Y. Hirabayashi, S.-A. T. E. Shioh, S. Sugii, and S. A. Summers. 2016. Adipocyte Ceramides Regulate Subcutaneous Adipose Browning, Inflammation, and Metabolism. *Cell Metab* **24**: 820-834.
56. Boden, G. 2008. Obesity and free fatty acids. *Endocrinol Metab Clin North Am* **37**: 635-ix.
57. Koliwad, S. K., N. E. Gray, and J.-C. Wang. 2012. Angiopoietin-like 4 (Angptl4): A glucocorticoid-dependent gatekeeper of fatty acid flux during fasting. *Adipocyte* **1**: 182-187.
58. Eseberri, I., J. Miranda, A. Lasa, I. Churrua, and M. P. Portillo. 2015. Doses of Quercetin in the Range of Serum Concentrations Exert Delipidating Effects in 3T3-L1 Preadipocytes by Acting on Different Stages of Adipogenesis, but Not in Mature Adipocytes. *Oxid Med Cell Longev* **2015**: 480943.
59. Lee, S. G., J. S. Parks, and H. W. Kang. 2017. Quercetin, a functional compound of onion peel, remodels white adipocytes to brown-like adipocytes. *J Nutr Biochem* **42**: 62-71.
60. Arias, N., C. Pico, M. Teresa Macarulla, P. Oliver, J. Miranda, A. Palou, and M. P. Portillo. 2017. A combination of resveratrol and quercetin induces browning in white adipose tissue of rats fed an obesogenic diet. *Obesity (Silver Spring)* **25**: 111-121.

61. Han, Y., J. Z. Wu, J. Z. Shen, L. Chen, T. He, M. W. Jin, and H. Liu. 2017. Pentamethylquercetin induces adipose browning and exerts beneficial effects in 3T3-L1 adipocytes and high-fat diet-fed mice. *Sci Rep* **7**: 1123.
62. Kuipers, E. N., A. D. V. Dam, N. M. Held, I. M. Mol, R. H. Houtkooper, P. C. N. Rensen, and M. R. Boon. 2018. Quercetin Lowers Plasma Triglycerides Accompanied by White Adipose Tissue Browning in Diet-Induced Obese Mice. *Int J Mol Sci* **19**.